

## Supporting Information

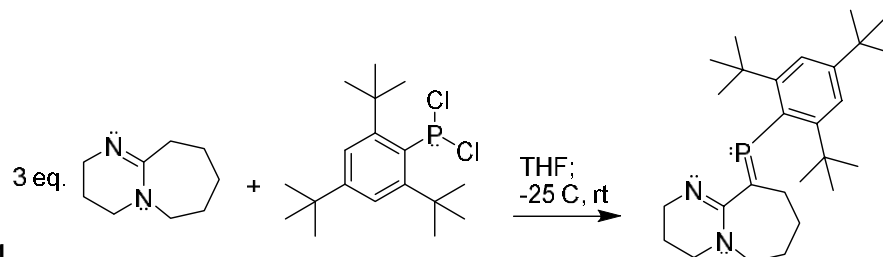
<b>Table of contents</b>	<b>S1</b>
<b>Technical details</b>	<b>S2</b>
<b>Synthesis</b>	<b>S3-S6</b>
<b>Fig. S1, Fig S2</b>	<b>S7</b>
<b>Fig. S3</b>	<b>S8</b>
<b>Fig. S4</b>	<b>S9</b>
<b>Fig. S5</b>	<b>S10</b>
<b>Fig. S6</b>	<b>S11</b>
<b>Fig. S7</b>	<b>S12</b>
<b>Fig. S8</b>	<b>S13</b>
<b>Fig. S9, Fig. S10, Fig S11</b>	<b>S14</b>
<b>Table S1</b>	<b>S15</b>
<b>Table S2</b>	<b>S16</b>
<b>NMR Experiments</b>	<b>S17-S21</b>
<b>Selected NMR Spectra</b>	<b>S22</b>
<b>References</b>	<b>S33</b>
<b>X-ray data</b>	<b>S34</b>

## Technical Details

DBU was bought from Sigma Aldrich, dried from calcium hydride and distilled under reduced pressure. THF (VWR) was dried from sodium/benzophenone and distilled under argon. The starting material 1,3,5-tri-tert-butylbenzene was bought from Sigma-Aldrich and used as received; the bromination to obtain Mes\*Br was synthesised according to a described procedure<sup>[1]</sup>. Ethereal hydrochloride (2M), HPF<sub>6</sub> (60% in H<sub>2</sub>O), and trifluoromethanesulfonic acid ReagentPlus<sup>®</sup>, ≥99% were bought from Sigma-Aldrich Acid and used fresh and as received. Deuterated solvents were obtained from Sigma Aldrich or Fluorochem and dried according to standard methods using molecular sieves. Anhydrous CDCl<sub>3</sub> was obtained from Sigma Aldrich. Other precursors were obtained from commercial suppliers and used without further purification. All reactions were performed under argon using Schlenk techniques. NMR measurements (<sup>1</sup>H, <sup>13</sup>C, <sup>15</sup>N and <sup>31</sup>P) were performed on a JNM-ECZ400S/L1 JEOL 400 MHz spectrometer and analysed with either Delta software (Jeol) or a licensed version of Mestrenova 12.01. Chemical shifts (<sup>1</sup>H, <sup>13</sup>C) are reported as δ values (ppm) relative to residual solvent signals. <sup>31</sup>P NMR spectra were recorded at 162 MHz with 85% H<sub>3</sub>PO<sub>4</sub> as an external reference. <sup>15</sup>N NMR spectra were recorded at 41 MHz with nitromethane as an external reference. The type of signal is abbreviated as follows: s = singlet, d = doublet, , br=broad, m = multiplet. Since most multiplet signals correspond to poorly-resolved pentets, they are reported as peaks on the centre of the resonance, or where the most intense signal occurs (e.g. Mes\*-H+DBU-CH<sub>2</sub>). Unless well-resolved, pentets corresponding to DBU-CH<sub>2</sub> signals are reported as multiplets. In 2d-phase-sensitive spectra (e.g. H, red contours correspond to positive intensities and blue to negative ones. Unless otherwise noted, due to low-solubility of certain compounds, <sup>13</sup>C NMR was not able to resolve quaternary carbons in some instances and was replaced by other indirect methods where appropriate. High-resolution mass spectra were measured using FTMS + p APCI or FTMS + p NSI (OrbitrapXL) at the University of Münster or our laboratory using ESI in the positive mode in a Bruker spectrometer. FTIR spectroscopy was performed in a PerkinElmer Spectrum One FT-IR spectrometer in transmittance mode, and the data's baseline subtracted using the spectrometer's software unless otherwise noted; after, spectra were analysed with EssentialFTIR and Origin 2016. For all experiments, 32 scans and a resolution of 2 cm<sup>-1</sup> were used as main parameters. Since the experimental conditions were almost identical for all samples, the nature of the compounds is structurally similar, and the transmittance mode was used (thus some spectral bands are more intense relative to others), a normalization of the spectra was done by in order to compare the data qualitatively, and it's is a valid approach for observing peak position changes as well as new or absent resonances; we limit discussions on relative changes in intensity to those samples that were measured under strictly similar conditions. Elemental analyses were performed at Analytical Laboratories, Prof. Dr. H. Malissa and G. Reuter GmbH, Germany. DFT analyses were performed using Gaussian 09 revision D.01 software. For most attempted calculations, B3LYP with GD3 dispersion correction, counterpoise corrections, and 6-311++G(2d,2p) as the basis set were used. The failure to optimise the dimeric structure at the DFT level is not caused by the Mes\* groups as we failed to optimise small model systems.

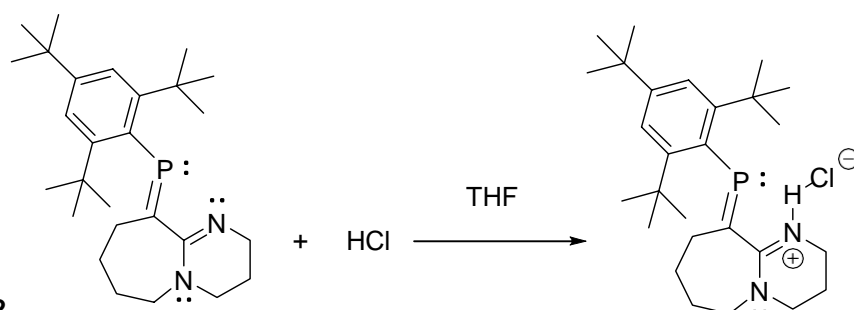
## Experimental

### Synthetic Work



#### Synthesis of 1

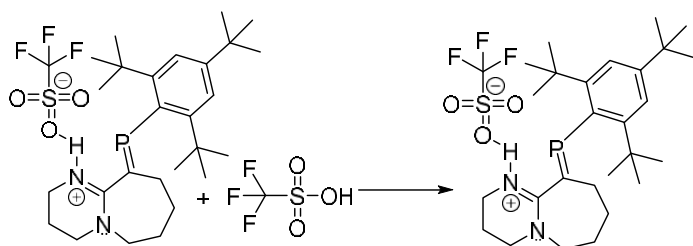
A slightly modified procedure than that reported previously was used. To a solution of dichloro(2,4,6-tri-tert-butylphenyl)phosphane (2.14 g, 6.16 mmol, 1 eq.) in THF (35 mL), previously dried & degassed DBU (2.86 mL, 19.1 mmol, 3.1 eq.) was added dropwise at  $-25\text{ }^{\circ}\text{C}$ . The reaction mixture sequentially changed from light yellow to dark yellow to lemon-lime, after addition of the three equivalents of DBU. The crude THF solution was concentrated under vacuum, digested into 15 mL of toluene, filtered through a Schlenk-frit and concentrated under vacuum (2.35 g, % 90). To the resulting solid which may still contain DBU-HCl as an impurity in some batches, cold freshly distilled (under argon) acetonitrile (3 mL x 2) was gently added under inert conditions; the mixture was gently swirled for 2 minutes while keeping a slight argon overpressure to avoid air/moisture contamination. Subsequently, the acetonitrile supernatant was decanted (the washing with acetonitrile is done twice), yielding **1** in (1.76 g, 75%) as a colourless powder. In agreement with literature data (see MS):  $^1\text{H}$  NMR (400 MHz, Chloroform -*d*)  $\delta$  7.35 (s, 2H), 3.46 (m, 2H), 3.19 (m, 2H), 3.05 (m, 2H), 1.80 (m, 2H), 1.72 (m, 2H), 1.51 (m, 2H), 1.42 (m, 2H), 1.32 (m, 2H), 1.24 (m, 2H).  $^{31}\text{P}$  NMR ( $\text{CDCl}_3$ , 162 MHz,)  $\delta$  (ppm): 257.9.  $^{15}\text{N}$  NMR (41 MHz, Chloroform -D)  $\delta$ : -318 (amine), -189 (imine). HRMS (FTMS + p NSI): 427.32343 m/z [( $\text{C}_{27}\text{H}_{43}\text{N}_2\text{P}$ )+H] (calcd for [( $\text{C}_{27}\text{H}_{43}\text{N}_2\text{P}$ )+H]: 427.32421).



#### Synthesis of 2

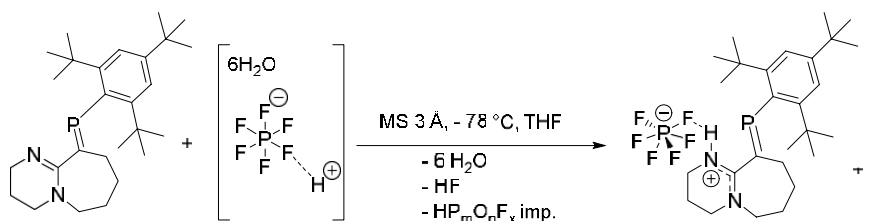
For **2**-hydrogen-bonded or **2**· $\text{H}_2\text{O}$  see later. In a typical experiment, **1** was dissolved in THF under inert conditions; then the mixture was reacted with  $\sim 1.1$  equivalents of anhydrous ethereal HCl (2M), quantitatively yielding **2**. To obtain extremely pure **2** for H-bonding experiments, the mixture can be washed with pentane and toluene and filtered (removal of grease may be difficult).  $^1\text{H}$  NMR (400 MHz, Chloroform-*d*)  $\delta$  11.14 (s, 1H), 7.40 (s, 2H), 3.80 – 3.72 (m, 2H), 3.49 (m, 2H), 3.35 – 3.28 (m, 2H), 2.07 (m, 2H), 1.79 – 1.66 (m, 2H), 1.53 (s, 19H), 1.31 (s, 11H).  $^{13}\text{C}$  NMR (101 MHz, Methylene chloride-*d*<sub>2</sub>)  $\delta$  122.51, 52.12, 48.63, 39.59, 33.48 (d,  $J = 7.1$  Hz), 32.54 (d,  $J = 13.3$  Hz), 30.98, 24.67, 24.01 (d,  $J = 3.8$  Hz), 19.99.  $^{31}\text{P}$  NMR (162 MHz, Chloroform-D)  $\delta$  311.52. HRMS (ESI,  $\text{CH}_3\text{CN}$ , + mode): 427.32215 m/z [( $\text{C}_{27}\text{H}_{43}\text{N}_2\text{P}$ )+H-Cl] (calc. for [( $\text{C}_{27}\text{H}_{43}\text{N}_2\text{P}$ )+H-Cl]: 427.32421). Due to either low T2, or low solubility, a satisfactory 1D- $^{13}\text{C}$ -NMR could not be obtained. However,  $^1\text{H}$ - $^{13}\text{C}$  HSQC,  $^1\text{H}$ - $^{13}\text{C}$  HMBC, a very clean  $^1\text{H}$ - $^{13}\text{C}$  DEPT-135, in addition to other techniques unanimously proved the structure of **2**.

### Synthesis of 3



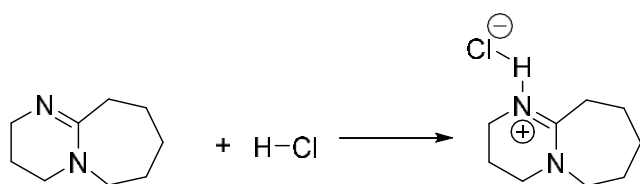
A slightly modified procedure than that for **2** was used. In a typical reaction, to a solution of **1** (0.194 g, 455  $\mu\text{mol}$ ) in 10 mL of THF charged with 3 Å MS at  $-78^\circ\text{C}$ , triflic acid (42  $\mu\text{mol}$ , 475  $\mu\text{mol}$ ) was added. The mixture was filtered under a nitrogen atmosphere, swirled in 2 mL of  $\text{CH}_3\text{CN}$ , decanted, washed with hexanes and pentane, in order to obtain **3** as a colorless powder (80% yield).  $^1\text{H}$  NMR (400 MHz, Chloroform- $d$ )  $\delta$  8.67 (s, 1H), 7.40 (s, 2H), 3.68 (s, 2H), 3.55 (s, 1H), 3.34 (s, 1H), 2.12 (s, 1H), 1.74 (s, 1H), 1.59 (s, 1H), 1.31 (s, 6H).  $^{13}\text{C}$  NMR (101 MHz, Chloroform- $d$ )  $\delta$  170.11 (d,  $J = 49.7$  Hz), 164.46 (d,  $J = 29.9$  Hz), 154.31, 151.80, 131.75 (d,  $J = 59.0$  Hz), 122.64, 52.53, 48.65, 39.76, 38.14, 35.15, 33.54 (d,  $J = 6.7$  Hz), 32.49 (d,  $J = 13.0$  Hz), 31.36, 24.04, 19.91, 15.37.  $^{19}\text{F}$  NMR (376 MHz, Chloroform- $d$ )  $\delta$  -78.07.  $^{31}\text{P}$  NMR (162 MHz, Chloroform- $d$ )  $\delta$  310.18. HRMS (ESI,  $\text{CH}_3\text{CN}$ , + mode): 427.32295 m/z  $[(\text{C}_{27}\text{H}_{43}\text{N}_2\text{P})+\text{H}-\text{SO}_3\text{CF}_3]$  (calc. for  $[(\text{C}_{27}\text{H}_{43}\text{N}_2\text{P})+\text{H}-\text{SO}_3\text{CF}_3]$ : 427.32421)

### Synthesis of 4



A slightly modified procedure than that for **2** was used. In a typical reaction, to a solution of **1** (0.015 g, 35  $\mu\text{mol}$ ) in 3 mL of THF charged with 3 Å MS at  $-78^\circ\text{C}$ ,  $\text{HPF}_6$  (60%, 10  $\mu\text{L}$ , 70  $\mu\text{mol}$ ) was added. The mixture was filtered under a nitrogen atmosphere, swirled in 2 mL of  $\text{CH}_3\text{CN}$ , decanted, washed with hexanes, in order to obtain 15 mg of **4** as colorless powder (75% yield).  $^1\text{H}$  NMR (400 MHz, Chloroform- $d$ )  $\delta$  7.56 (s, 1H), 7.43 (s, 2H), 3.87 (m, 2H), 3.68 (m, 2H), 3.58 (m, 2H), 3.38 (m, 2H), 2.16 (m, 2H), 1.77 (m, 2H), 1.62 (m, 2H), 1.48 (m, 18H), 1.32 (m, 11H).  $^{31}\text{P}$  NMR (162 MHz, Benzene- $d_6$ )  $\delta$  301.58, -143.43 (hept,  $J = 710.2$  Hz).  $^{13}\text{C}$  NMR (101 MHz, Chloroform- $d$ )  $\delta$  170.87 (d,  $J = 50.2$  Hz), 164.50 (d,  $J = 29.4$  Hz), 154.24, 151.94, 131.32 (d,  $J = 58.1$  Hz), 122.74, 52.87, 48.65, 40.14, 38.13, 35.14, 33.52 (d,  $J = 6.1$  Hz), 32.51 (d,  $J = 12.0$  Hz), 31.33, 25.72, 24.29 (d,  $J = 54.0$  Hz), 19.75.  $^{19}\text{F}$  NMR (376 MHz, Benzene- $d_6$ )  $\delta$  -73.23 (d,  $J = 710.2$  Hz). HRMS (ESI,  $\text{CH}_3\text{CN}$ , + mode): 427.32248 m/z  $[(\text{C}_{27}\text{H}_{43}\text{N}_2\text{P})+\text{H}-\text{PF}_6]$  (calc. for  $[(\text{C}_{27}\text{H}_{43}\text{N}_2\text{P})+\text{H}-\text{PF}_6]$ : 427.32421).

## Synthesis of 5

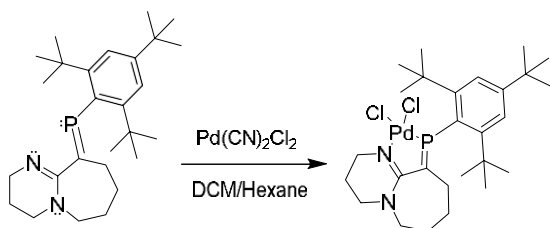


The non-phosphaalkene containing species **5** was synthesized by adding 1.2 equivalent of HCl (2M in THF) to a solution of DBU in THF, which was thoroughly dried.  $^1\text{H}$  NMR (400 MHz, Chloroform-*d*)  $\delta$  11.08 (s, 1H), 3.50 (m, 4H), 3.38 (m, 2H), 2.93 (m, 2H), 2.00 (p, 2H), 1.72 (m, 4H), 1.67 (m, 2H).  $^{13}\text{C}$  NMR (101 MHz, Chloroform-*d*)  $\delta$  166.38, 54.59, 48.88, 38.04, 32.31, 28.97, 26.85, 24.07, 19.64.  $^1\text{H}$ - $^{15}\text{N}$  HMBC NMR (400 MHz, Chloroform-*d*)  $\delta$  -282.11, -287.20.

## Single Crystals of 1, 2·H<sub>2</sub>O, 3, 4 and 5:

The single crystals were obtained from diffusion of *n*-hexane into concentrated solutions of dissolved materials in  $\text{CH}_2\text{Cl}_2$ .

## Single Crystals of 6



**1** (50 mg, 0.12 mmol) and  $\text{Pd}(\text{MeCN})_2\text{Cl}_2$  (1 eq., 0.12 mmol) were mixed in dichloromethane and stirred for 1 h under an argon stream. The resulting mixture was filtered through a celite pad. The resulting solution layered with hexane and kept for crystallisation. After several weeks single crystals (orange) were obtained.  $^1\text{H}$  NMR (400 MHz, Chloroform-*d*)  $\delta$  7.56 (d,  $J=3.6$  Hz, 2H), 4.08 (m, 2H), 3.52 (m, 2H), 3.38 (m, 2H), 2.03 (m, 2H), 1.94 (m, 2H), 1.85 (m, 2H), 1.68 (m, 18H), 1.53 (m, 2), 1.33 (m, 9H).  $^{31}\text{P}$  NMR (Chloroform-*d*, 162 MHz,)  $\delta$  (ppm): 249.00 (b). HRMS (FTMS + p NSI): 1045.47725  $m/z$  [(2L+1M)+(OH)] (calcd for [(2L+1M)+(OH)]: 1045.47670). Due to unidentified DBU impurities typical of these products, a suitable  $^{13}\text{C}$ -NMR could not be obtained. However, a  $^1\text{H}$  NMR, a single-crystal X-ray structure, plus high-resolution-mass-spectroscopy confirm the synthesis of **6**.

## Synthesis of 2·H<sub>2</sub>O

Method 1: Once **2** was obtained under inert conditions, the formation of **2·H<sub>2</sub>O** was done by adding a stoichiometric amount of  $\text{H}_2\text{O}$  using a Hamilton syringe or a 10 M  $\text{H}_2\text{O}$  solution in THF which was then evaporated.

Method 2: Once **2** was obtained under inert conditions, single crystals of **2·H<sub>2</sub>O** were obtained from diffusion of *n*-hexane into concentrated solutions of the dissolved material in  $\text{CH}_2\text{Cl}_2$ .

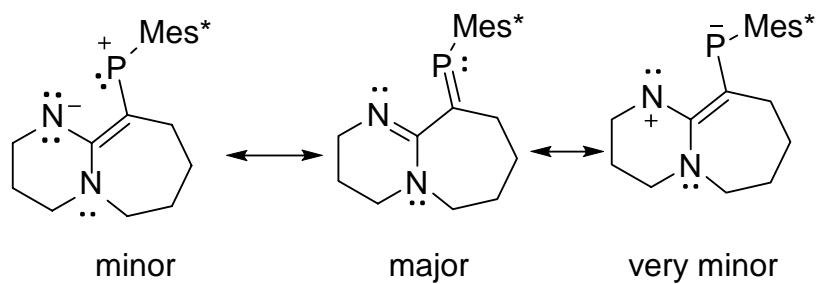


Figure S1. Possible resonance structures of **1**. Contributions to the electronic structure are indicated in the figure.

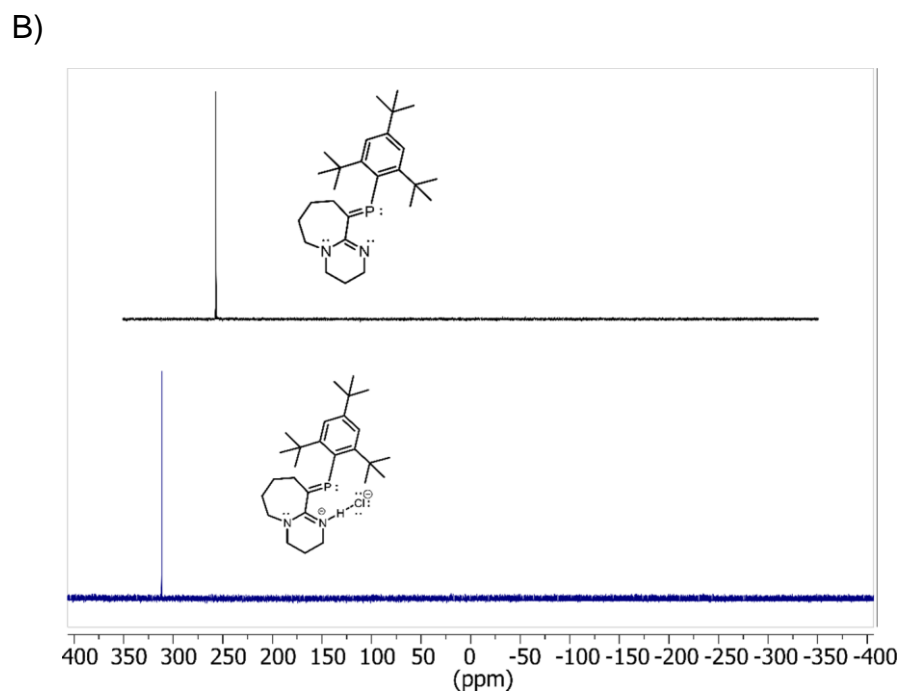
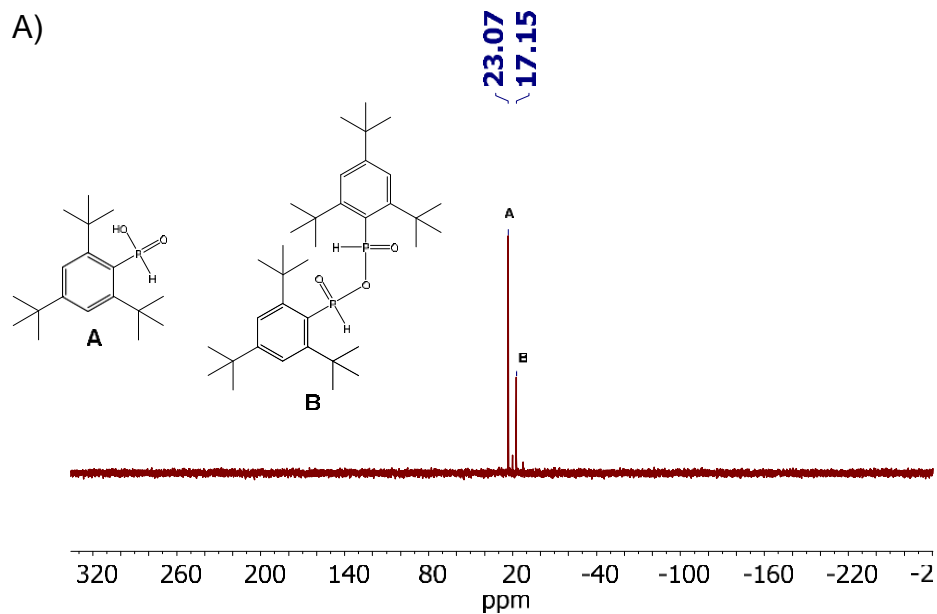


Figure S2. A) Observed decomposition products of **1** after 6 hours of exposure to the atmosphere by opening Schlenk flask. Solvent: toluene (NMR lock: inner Benzene- $d_6$  capillary tube). Assignments were

based on previous references.<sup>[3]</sup> B) Selected  $^{31}\text{P}$  NMR spectra monitoring the reaction from **1** (top) to **2** (bottom), solvent ( $\text{CDCl}_3$ ).

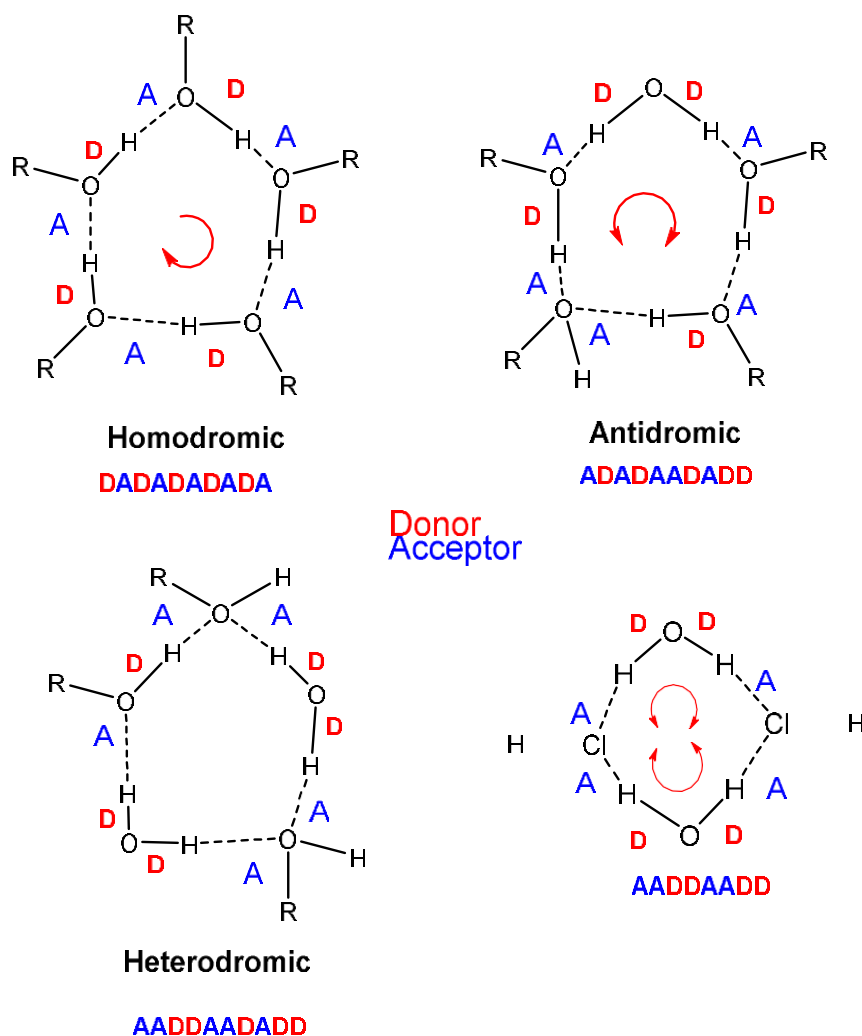


Figure S3. Different types of hydrogen bonding in a cyclic ring. A) Homodromic: the direction of donor-acceptor connectivity closes the ring. B) Antidromic: the direction of donor-acceptor connectivity goes in opposite direction and cancels one another at one endpoint on the ring. C) Heterodromic: no sense of direction. D) In this work, ( $2 \cdot \text{H}_2\text{O}$ ) a cyclic heteroatomic (i.e. O and Cl) quadrilateral type of network is envisioned, and it does not follow the typical definition of homodromic or heterodromic hydrogen bonding. To determine the novelty of the presented ring arrangement, a structure search was performed on ConQuest 1.19 in the Cambridge Crystallographic Database by restricting the search to the presented ring arrangement, with two water molecules acting as four proton donors only and two chloride ions acting as acceptors of three hydrogens only. Atomatically speaking, the ring is not novel, but in the other ones, water is either acting as an acceptor also, or the chlorides are acceptors of more than three protons. Therefore, the novelty of the presented arrangement lies in the fact that the water molecules are donors only, and the chloride is an acceptor of three protons only, forming a discrete halogen/water mixture.

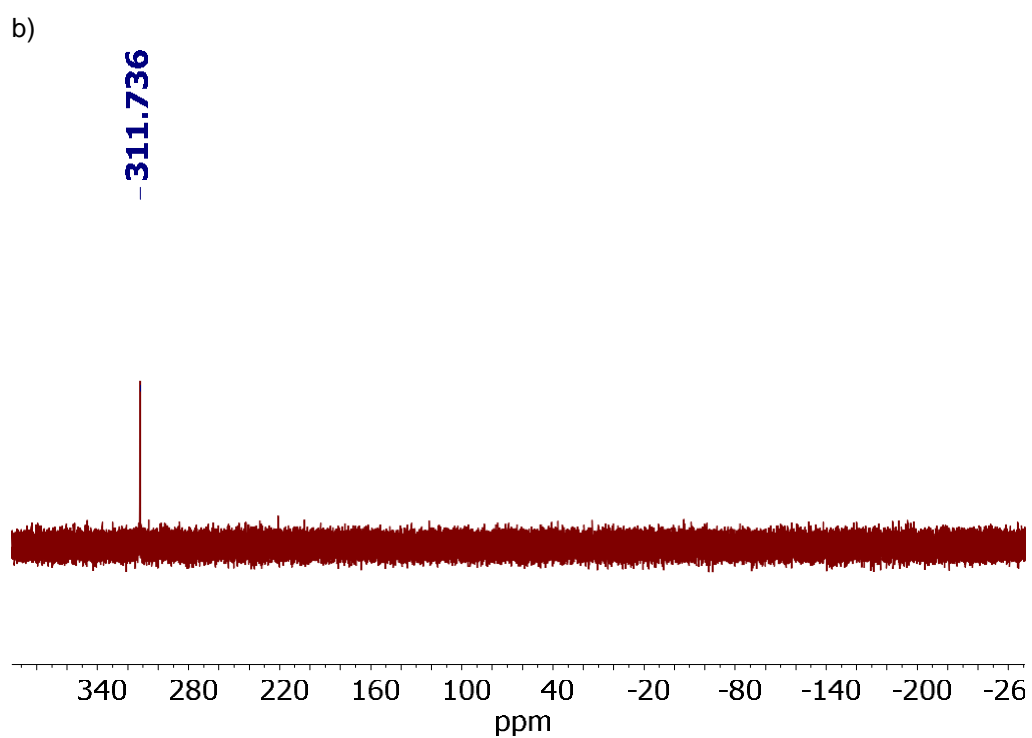
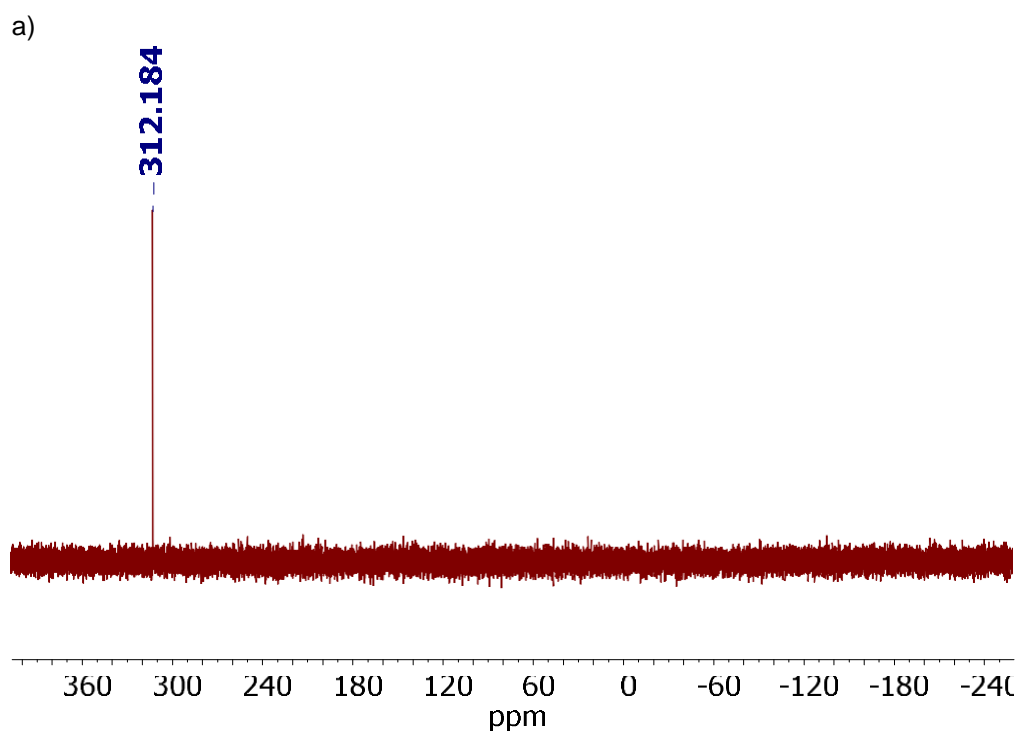


Figure S4. Selected  $^{31}\text{P}$  NMR spectra of **2** a) Day 1 b) Day 30. NMR tube opened to atmosphere, occasionally refilled during the 30-day span, including before measuring the shown spectrum at Day 30. No other visible impurities.

Compound	P1-N1-H1-Cl1	P1-N2-H1-Cl1	P1-H3-Cl1-P2	P1-O2-Cl1-Cl2	P1-Cl1-Cl2-P2	P1-O1-Cl2-O2	P1-N4-N1-P2	P1-N2-H6-N3	N1-P2-O1-N2
<b>2·H<sub>2</sub>O</b>	-158.40	167.56	-9.64	179.55	180.00	0.26	-180	13.97	-15.17

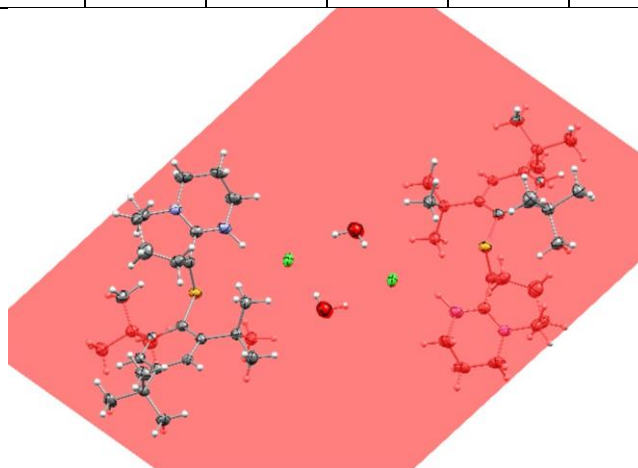


Figure S5. ORTEP representation of **2·H<sub>2</sub>O** and the least squares plane (through the quadrilateral water arrangement). Note that the phosphorus chlorine distances are significantly above the sum of their VdW  $r_i$  (3.55 Å). It is imperative to note that further interactions as a whole induce directionality and may contribute to the formation of this remote dimeric water cluster encumbered by a hydrophobic environment.

**FT-IR and FT-ATR-IR Spectroscopy Experiments:** Infrared spectroscopy was used to reveal the presence of hydrogen bonding in **2** and **2·H<sub>2</sub>O**, based on key vibrational frequencies. For the dimer **2·H<sub>2</sub>O**, two discrete OH- stretches with the same intensities, from supramolecular hydrogen-bonded water-containing species are expected, as opposed to the OH- resonance seen in species with a relative excess water (e.g. water-clusters, aqueous solutions, water-containing nonaqueous mixtures, among others) which is broadened due to dynamic hydrogen bonding/breaking processes among water molecules. Very notably, we can notice how the spectrum of **2-anhydrous** (**b**) lacks any character corresponding to a supramolecular hydrogen bonded water molecule (>3200 cm<sup>-1</sup>), whereas the **2-diluted** (**c**) and **2-concentrated** (**d**), display hydrogen-bonded interactions at ~3450 cm<sup>-1</sup>. In terms of shape and intensity, the symmetry of the two signals in (**d**) clearly determine the formation of a dimeric species **2·H<sub>2</sub>O** with two H<sub>2</sub>O molecules in the same supramolecular environment, as better seen in e). The OH- stretches of a hydrogen bonded monomeric species display OH- resonances with unequal shapes and intensities due to the coordination of one of its water molecules only [2], which changes the nature of the resonances and specially their intensities. In (**f**), we can notice the dramatic changes on the regions containing the imine/iminium carbon stretches, iminium proton rocking. On the other hand, the presence of H-O-H bending (**g**) is completely obscured by the DCM resonances.

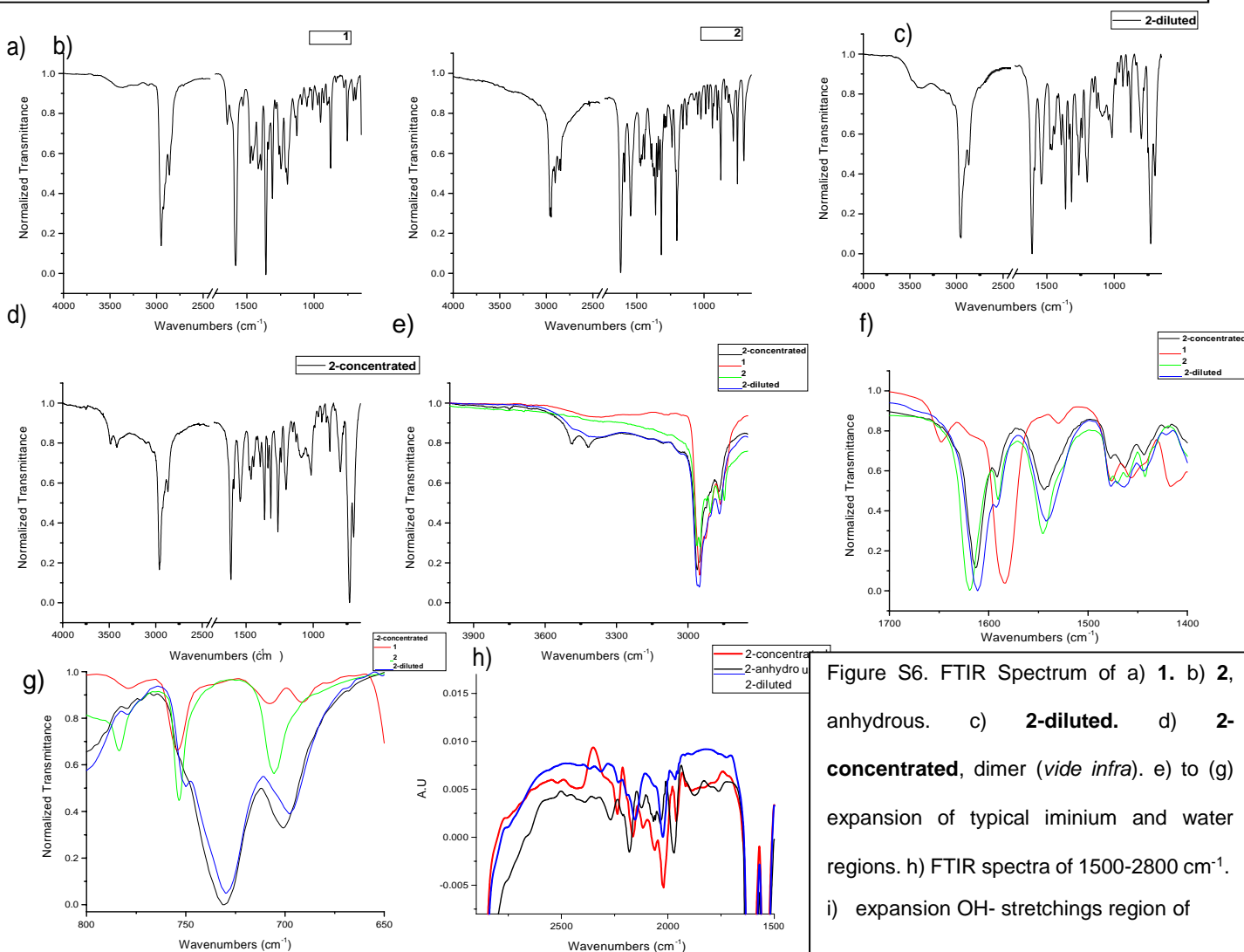


Figure S6. FTIR Spectrum of a) **1**. b) **2**, anhydrous. c) **2-diluted**. d) **2-concentrated**, dimer (*vide infra*). e) to (g) expansion of typical iminium and water regions. h) FTIR spectra of 1500-2800 cm<sup>-1</sup>. i) expansion OH- stretchings region of crystalline **2·H<sub>2</sub>O** (solid state, KBr pellet)

Spectra a)-h) were taken using the FT-ATR-IR technique. Spectra i) was taken using KBr pellets. In the case of **2-diluted** and **2-concentrated** 3 drops were carefully added on a previously cleaned and dried AT-IR crystal, which was immediately sealed, and the spectrum was taken within 30 seconds of the addition of the solvent. Preparation of **2-diluted**: around ~4 mg of **2** diluted in ~1 mL of slightly-wet DCM (0.5 % H<sub>2</sub>O). This mixture is less-likely to participate in hydrogen bonding owing to two different additive reasons. Reason 1) A more dilute mixture leads to less hydrogen bonding interactions between hydrogen-bonding donor/acceptors (i.e. N, Cl). Reason 2) A more dilute mixture in slightly wet DCM (~1 molecule of 2 per 3 molecules of water) experiences less hydrogen bonding from the larger amount of water relative to a concentrated mixture in the same batch of solvent. As seen in the spectrum, a single broad band with no discrete features indicate either a hydrogen bonding environment of a monomeric species or one in which the water excess is dictating the OH- IR character. Preparation of **2-concentrated**: around ~8 mg of **2** were added to the previous solution of DCM to make it three-times more concentrated and more likely to create the dimeric hydrogen-bonded network by having an approximate **2** to H<sub>2</sub>O equimolar ratio. The resulting spectrum with two discrete features at 3489 and 3419 cm<sup>-1</sup> corroborates the formation of **2·H<sub>2</sub>O**. The blank backgrounds remove CO<sub>2</sub> and water

vapour. After subtraction and even before smoothing, there were clear resonances, which in the solution samples do not seem to account for free CO<sub>2</sub>. Though speculative<sup>[4]</sup>, these bands, if corresponding to resonances instead of added noise, could indicate the presence of strong-hydrogen-bonded HCl (i.e. HB equilibrium towards HCl, either from iminium protons or water molecules, among other possibilities, see references) species in equilibrium, and DCM-hydrogen-bonded species<sup>[5]</sup>

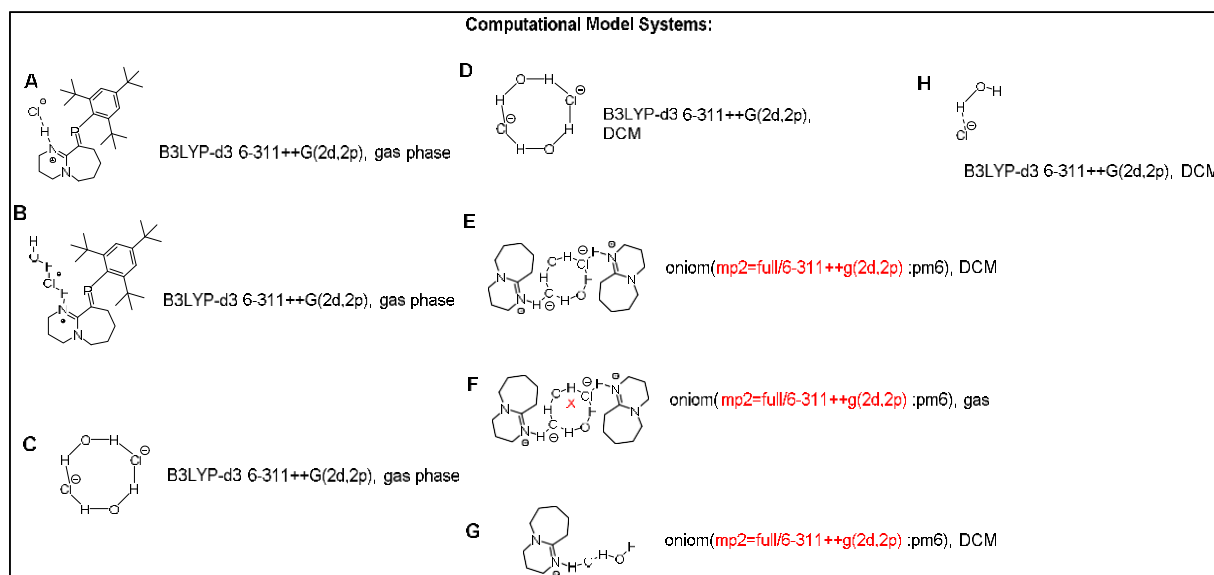
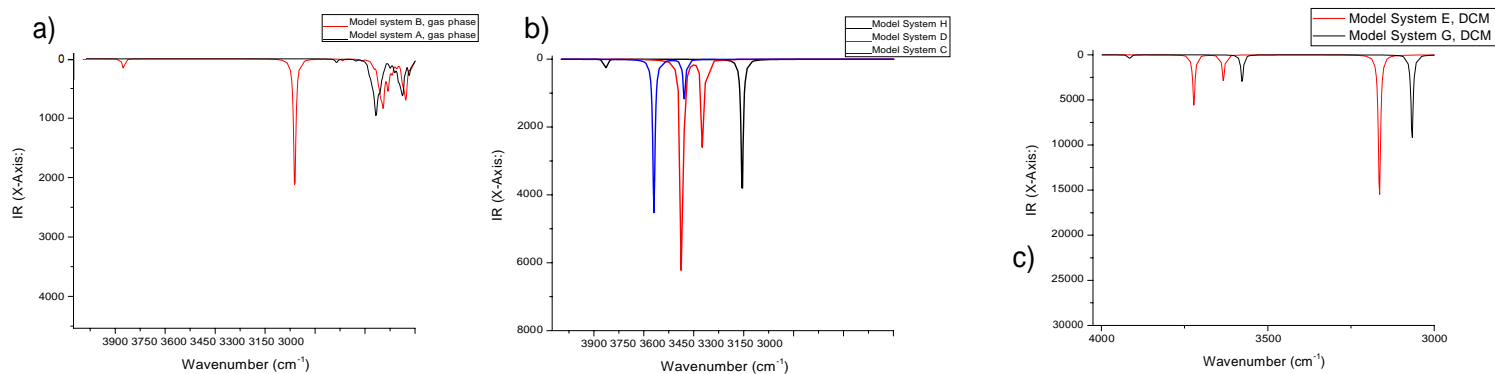


Fig. S7. The dimer  $2\cdot\text{H}_2\text{O}$  was not optimised successfully thus far, and even lower levels of theory resulted in prohibitively expensive files and long computation times with no seeming improvements. On the other hand, the monomeric-hydrate system, as well as the anhydrous one **2**, converged successfully; their IR spectrum was calculated successfully (See a-c) for calculated spectra). We then optimised and calculated the IR spectra of smaller monomeric and dimeric model systems. We then qualitatively analysed the -OH stretch region of interest for all of them as shown above. In the case of **2**-anhydrous, no stretch in the region of interest is present, confirming the experimental data. For the monomeric hydrogen bonded structure the stretching vibration of the OH involved in hydrogen bonding does not match with the experimentally observed bands as they occur more than  $500\text{ cm}^{-1}$  from each other as seen in (a), and as expected from simple principles. The smaller monomeric systems expectedly followed the same trend qualitatively. On the other hand, the dimeric modelled systems qualitatively present two -OH resonances which are as close to each other ( $< 100\text{ cm}^{-1}$ ) as those found experimentally for **2**-concentrated, thus confirming our assignment of it as the supramolecularly self-assembled  $2\cdot\text{H}_2\text{O}$ . System F in the gas phase yields a different structure in which only one of the chloride anions networks with the N-H motif and the water molecules, thus was not included in the analysis. The atoms on the mp2 layer were those that we considered being most important on the HB network and thus the FTIR analysis:  $(\text{N}_{\text{amine}}\text{-C-N}_{\text{amine}}\text{-H-Cl-H}_2\text{O})_2$ . The previous experimental data in combination with other published data, as well as our simple computational models serve as a basis for our assignment of **2**-concentrated as the dimeric species  $2\cdot\text{H}_2\text{O}$ . Since the DFT calculations were performed at the B3LYP-d3 6-311++G(2d,2p) level of theory, with Grimme's D3 dispersion correction.

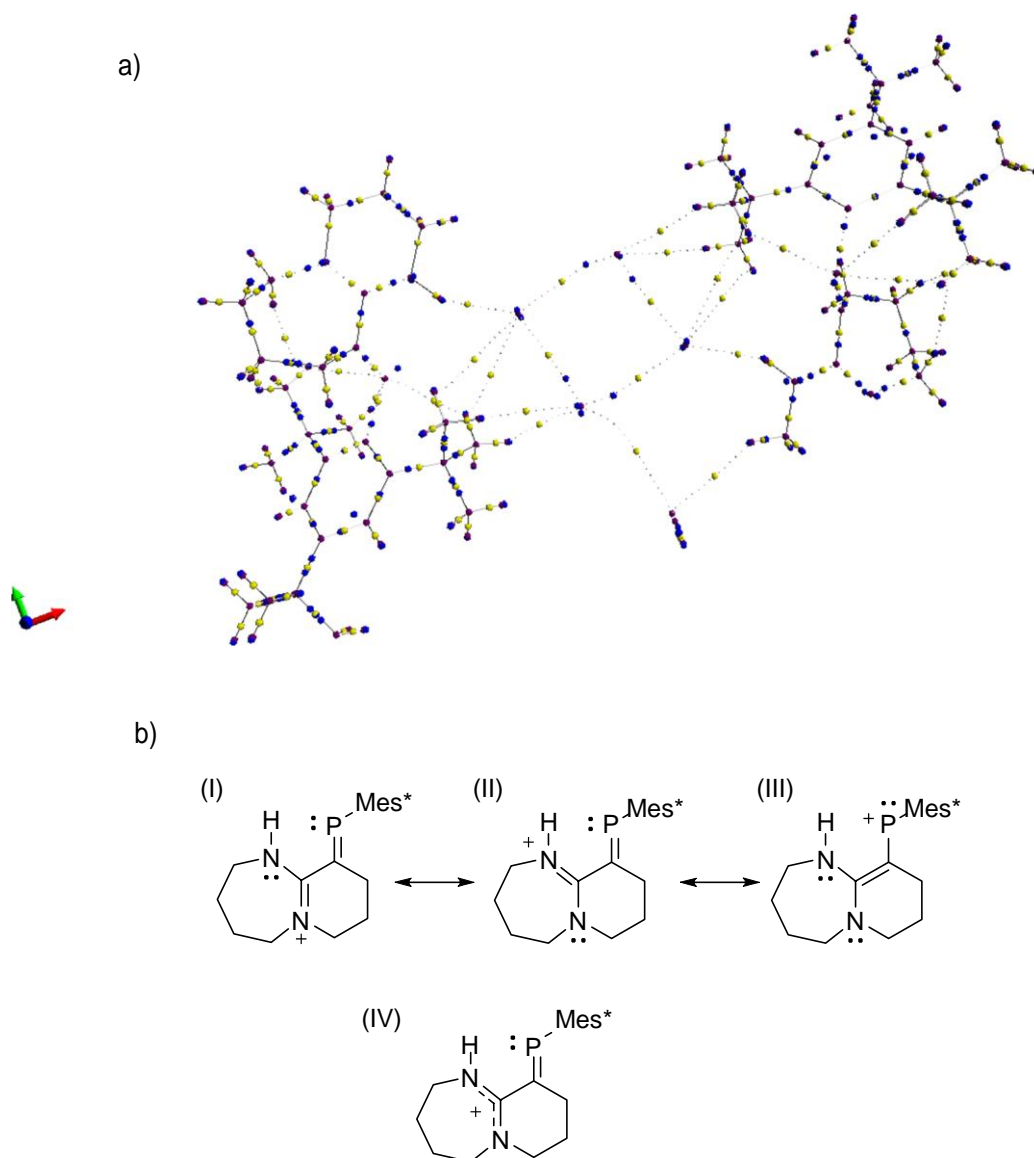


Fig. S8. a) Molecular graphs of **2**·**H<sub>2</sub>O** and smaller model systems (not shown) calculated using Atoms-In-Molecules (Bader) Analysis in Avogadro from a wavefunction containing the electronic density - **QTAIM**, yellow dots: bonds, blue dots: rings, thus confirming the hydrogen bonded ring network as described in the MS.

b) Possible resonance structures of the cationic fragments in **2 - 4**: (I) and (II) characterised by the cationic iminium and (III) by the cationic phosphonium centre, respectively. (IV) Resonance hybrid of (I) and (II) describing significant contributions to the overall delocalisation of the positive charge. Hydrogen-bonded adducts omitted for clarity.

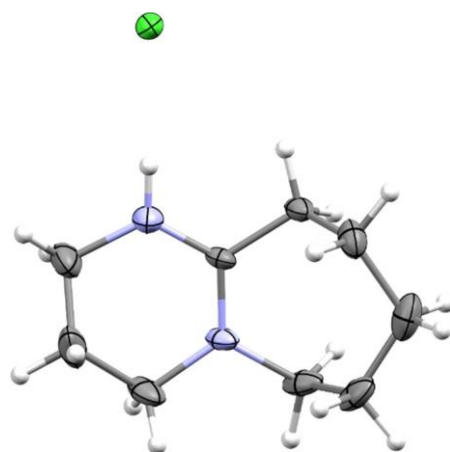


Figure S9. A) ORTEP representation DBU•HCl (**5**). (50% ellipsoids)

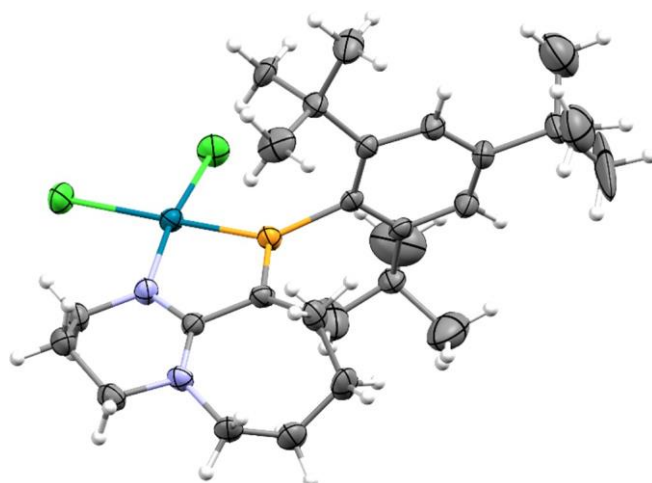


Figure S10. ORTEP representation of the Pd(II) complex **6**. (50% ellipsoids)

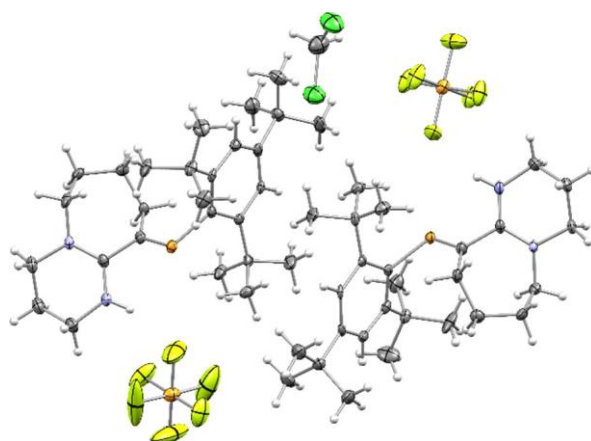
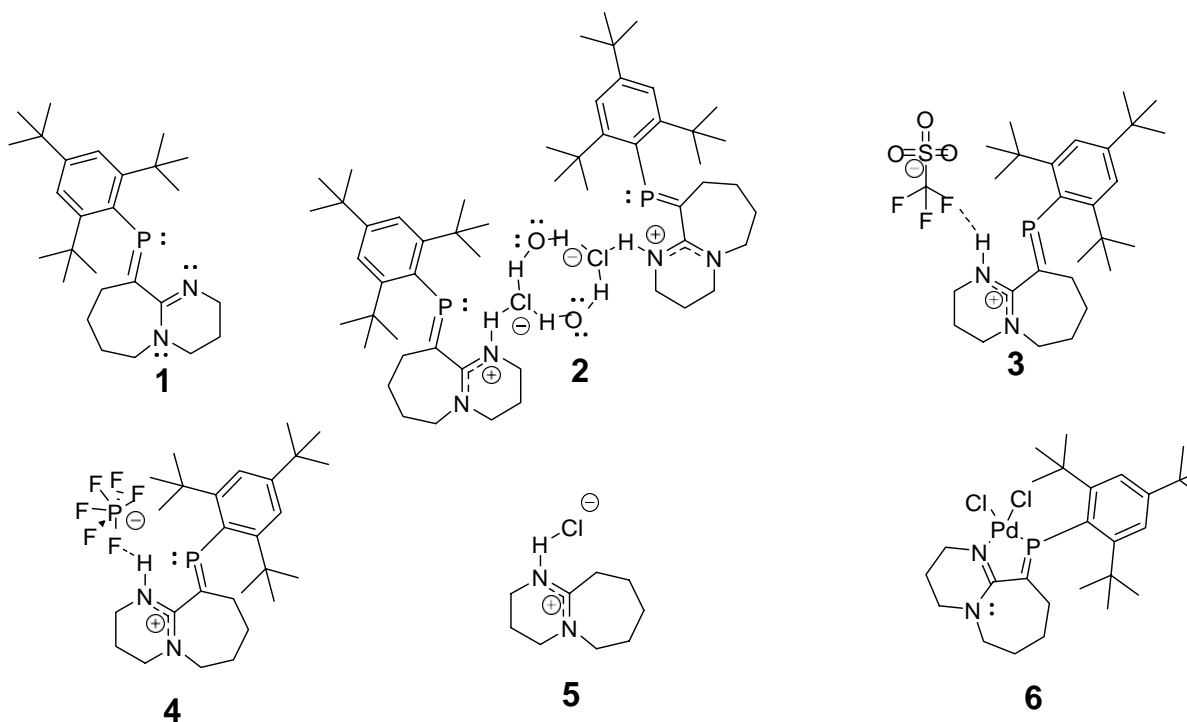
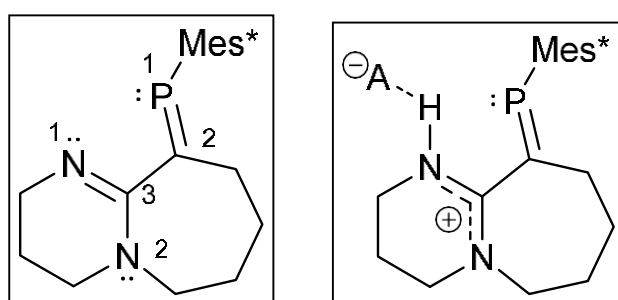


Figure S11. Asymmetric unit of **4**, ORTEP representation (50% ellipsoids).

Compound	P1-C2	N1-C3	N2-C3	C2-C3	P1-C2-C3-N1	P1-C2-C3-N2
<b>1</b>	1.676(3)	1.285(4)	1.370(4)	1.496(4)	55.4(3)	-126.6(3)
<b>2·H<sub>2</sub>O</b>	1.679(3)	1.325(4)	1.318(4)	1.479(4)	52.6(3)	-128.3(2)
<b>3</b>	1.689(4)	1.314(5)	1.329(5)	1.484(5)	-54.6(4)	126.7(3)
<b>4</b>	1.695(5)	1.311(7)	1.325(7)	1.503(8)	56.9(6)	-125.4(5)
	1.688(5)	1.314(7)	1.318(7)	1.485(8)	-56.4(6)	125.6(5)
<b>5</b>	n.a.	1.320(9)	1.317(7)	1.486(9)	-117(n.a.) <sup>a</sup>	116(n.a.) <sup>a</sup>
<b>6</b>	1.648(7)	1.321(8)	1.338(8)	1.480(9)	-12.3(7)	170.6(5)



**Table S1.** Selected bond length distances (Å) and angles (°) for compounds 1-6.

<sup>a</sup> the bisecting position of the methylene protons was used as “P1” to determine the dihedral angles.

Compound	D-A	DHA	Cl-O	Cl-H-O	Cl-O	Cl-H-O
<b>2·H<sub>2</sub>O</b>	3.097(3)	154(3)	3.302(3)	173(4)	3.203(3)	162(3)
<b>5</b>	3.156(6)	176				
<b>3</b>	2.980(9)	148(3)				
<b>4</b>	3.005(6) 2.932(7)	162(5) 152(5)				

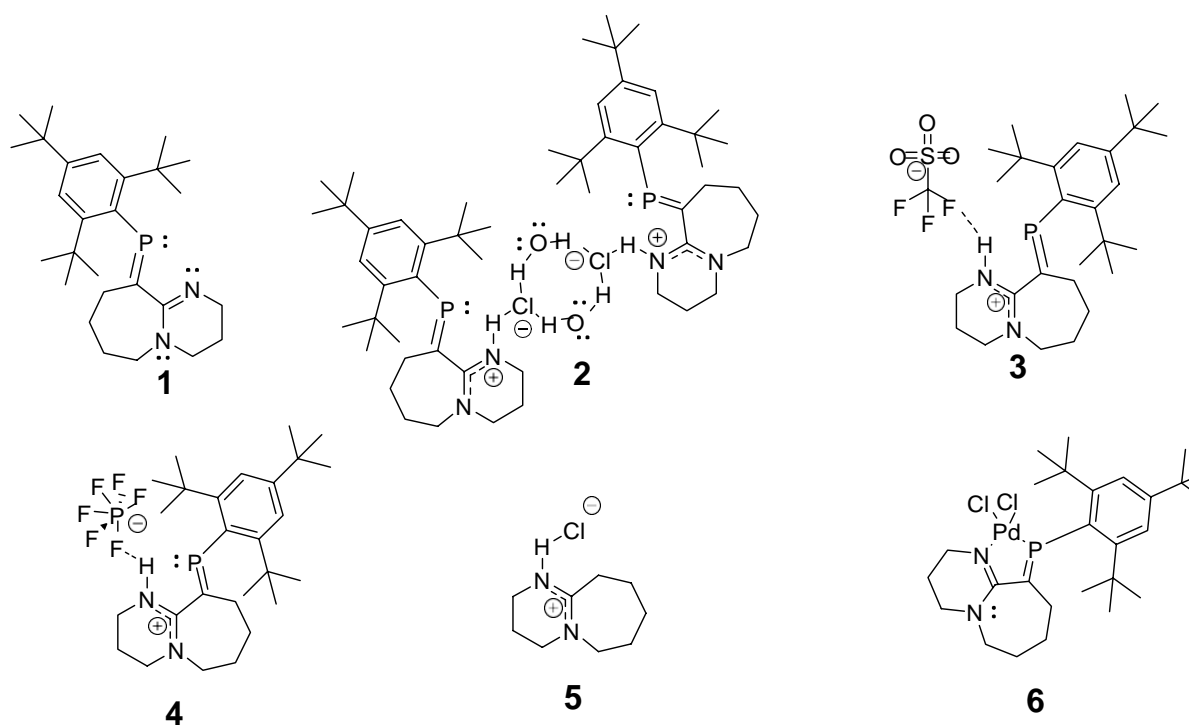
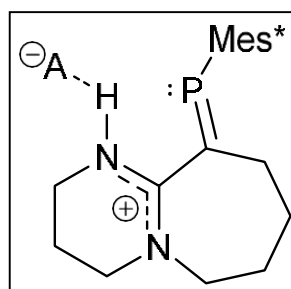
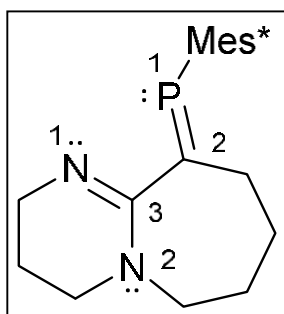


**Table S2.** Donor-Acceptor (D-A) hydrogen-bond length distances (Å) and angles (°) for compounds 1-6. As seen in the table, compound 4 crystallises with two molecules in the asymmetric unit cell.

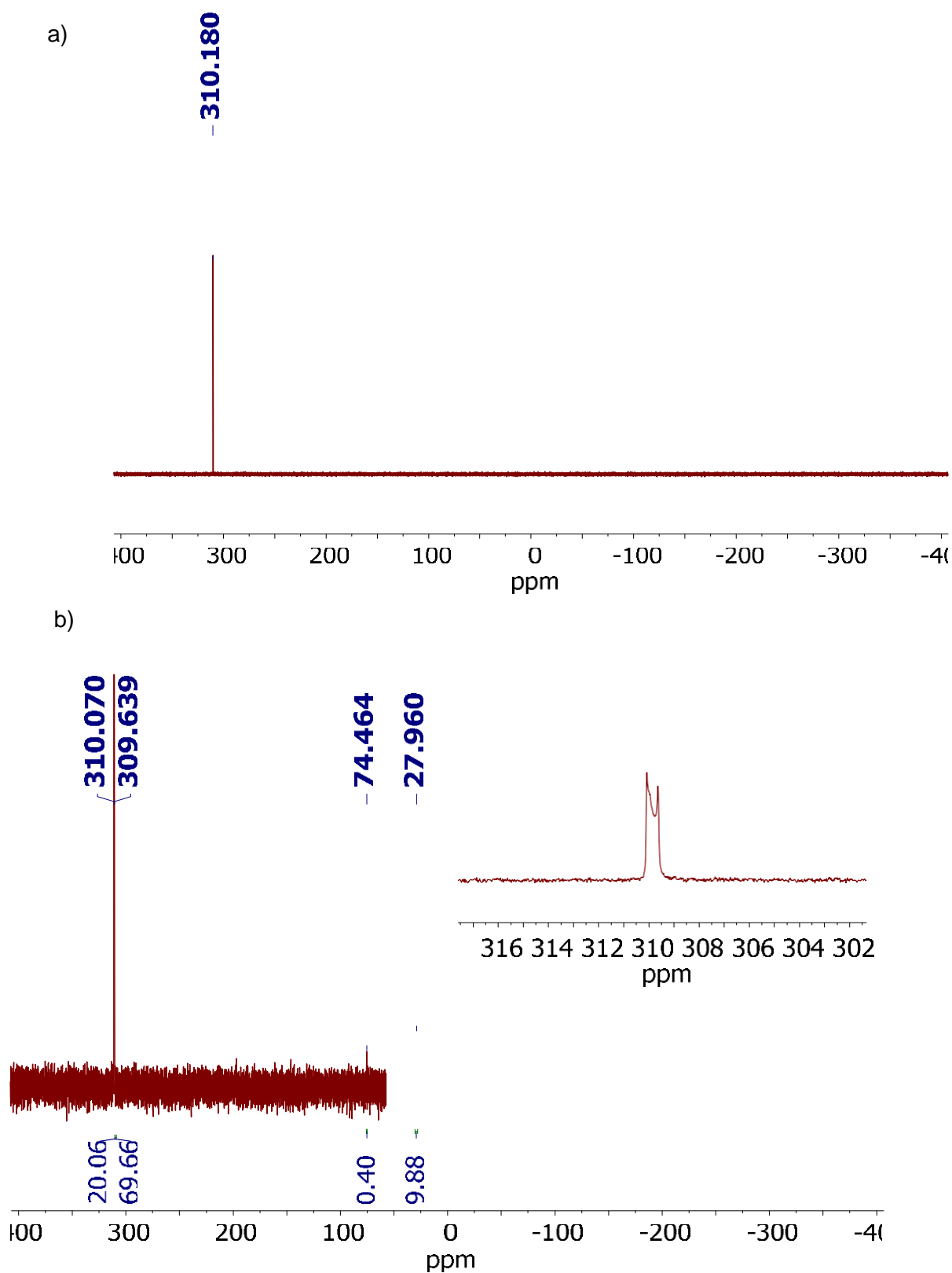
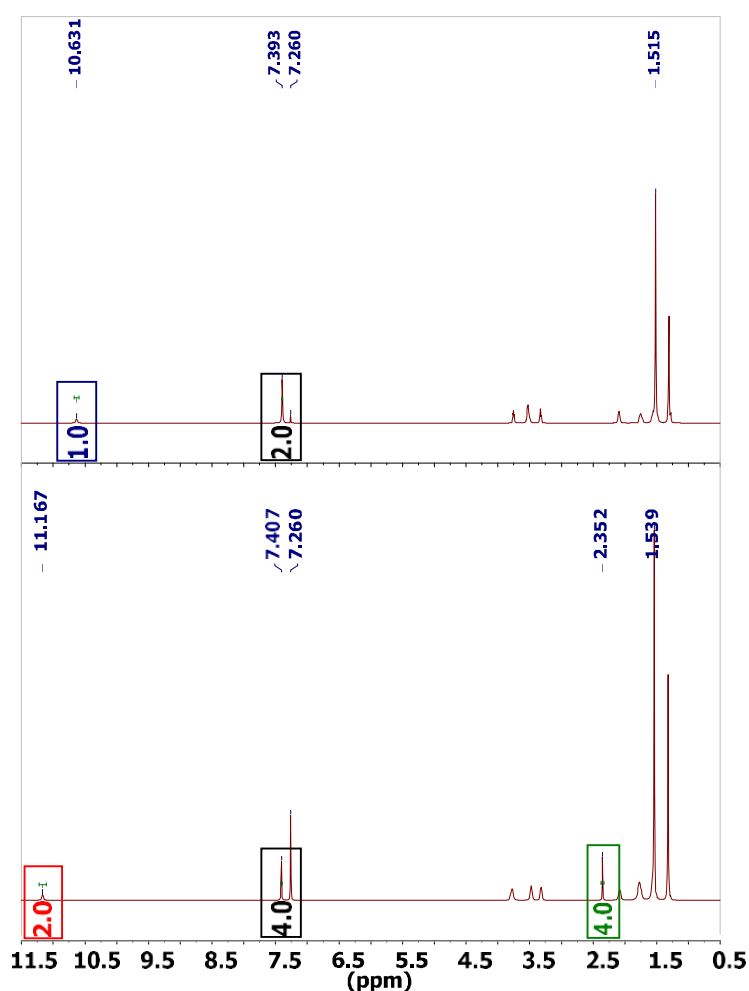


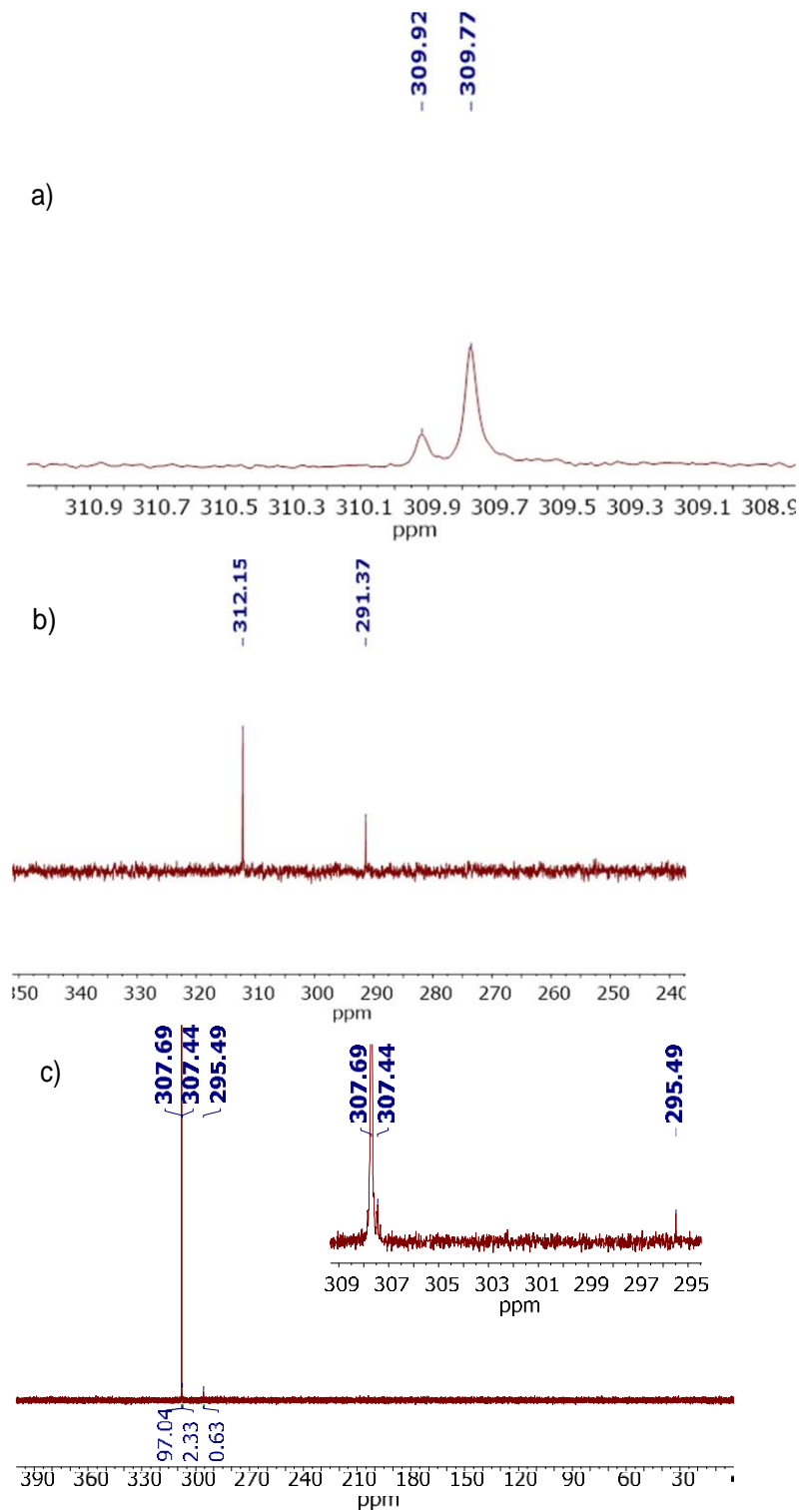
Figure S12. A) Selected  $^{31}\text{P}$  NMR spectra of **3** a) Freshly made b) NMR tube opened to atmosphere for eight days then refilled with deuterated solvent. Less than 10% visible impurities at 27.96 and 74.46 ppm. The lineshape of the signal in the phosphalkene region may be considered to support the presence of a hydrogen-bonded/ion-pair equilibria, nicely agreeing with previously observed data for **2**, (i.e. the increased water content and decomposition products in the latter spectrum decrease the hydrogen bond character between the imine nitrogen and the triflic acid oxygen species and shifts the equilibrium towards ion-pairs, at 309.64 ppm).

**Selected NMR experiments suggesting the formation of hydrogen-bonded species in solution. Attempts to probe  $2 \cdot \text{H}_2\text{O}$ , or, any hydrogen-bonding in solution (See Scheme below) as proof-of-principle within the heavy multiple bonded main-group chemistry regimes (i.e.  $\text{P}=\text{C}$ ):**

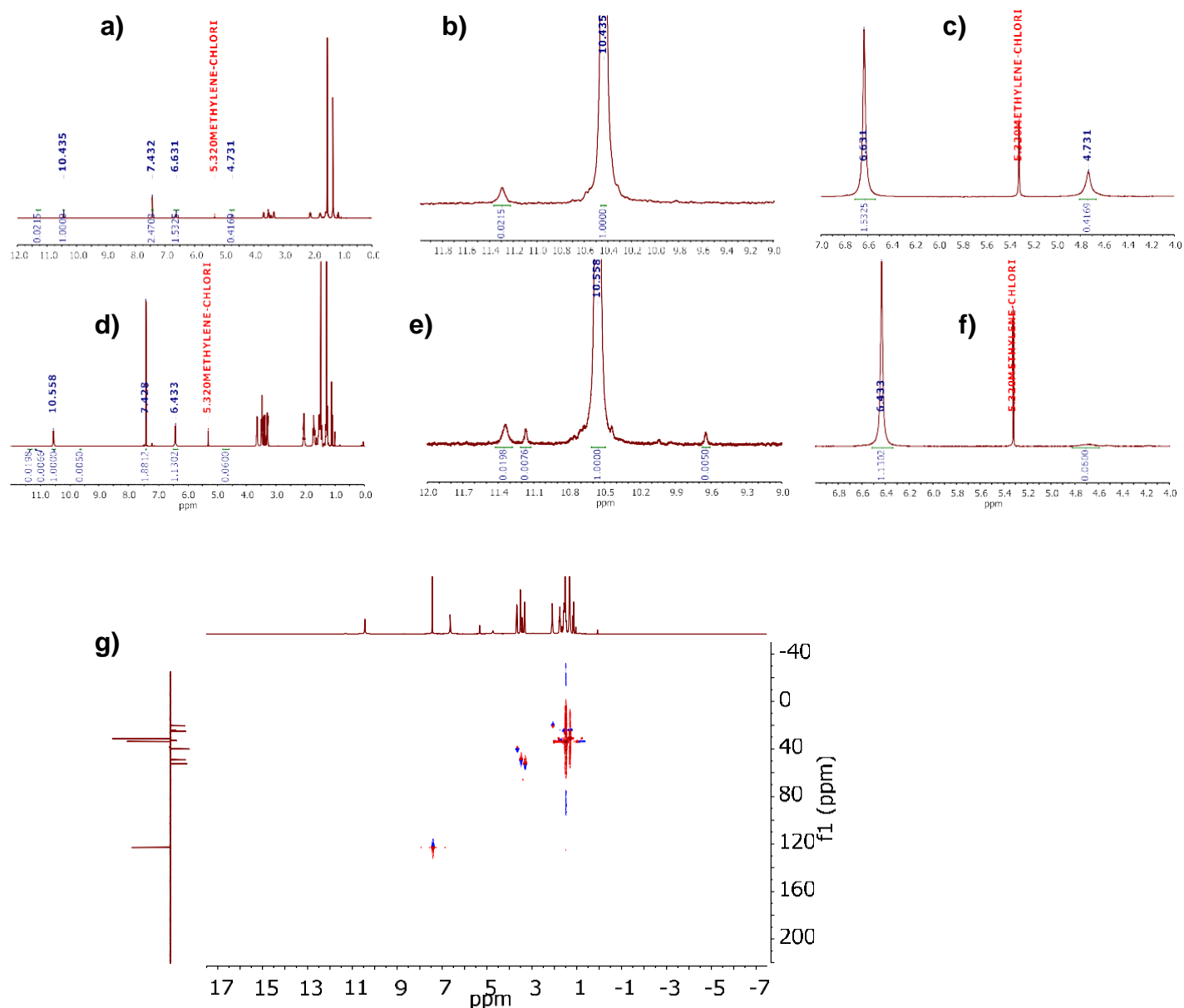
In a typical experiment, **1** was dissolved in THF under inert conditions; then the mixture was reacted with  $\sim 1.1$  equivalents of ethereal HCl (2M), quantitatively yielding **2** on a  $^{31}\text{P}$  NMR basis. In order to obtain ultrapure **2**, for hydrogen bonding experiments, the mixture can be washed with pentane and toluene repeatedly and collecting the product by filtering, or by carefully decanting or removing (with a syringe) the dirty solvent, then drying the resulting material under vacuum ( $5 \times 10^{-2}$  mbar) for more than 24 hours. Once **2** was obtained under inert conditions, the formation of  $2 \cdot \text{H}_2\text{O}$  was done by adding  $\text{H}_2\text{O}$  using a Hamilton syringe or a 10 M  $\text{H}_2\text{O}$  solution in THF (either stoichiometrically to form  $2 \cdot \text{H}_2\text{O}$  or in excess, depending on the goal of the experiment). Below each set of NMR spectra, a brief discussion of the presented experimental results is shown in the caption. The spectra were performed at room temperature unless otherwise noted. The spectra were processed using a licensed version of Mestrenova 12.01.



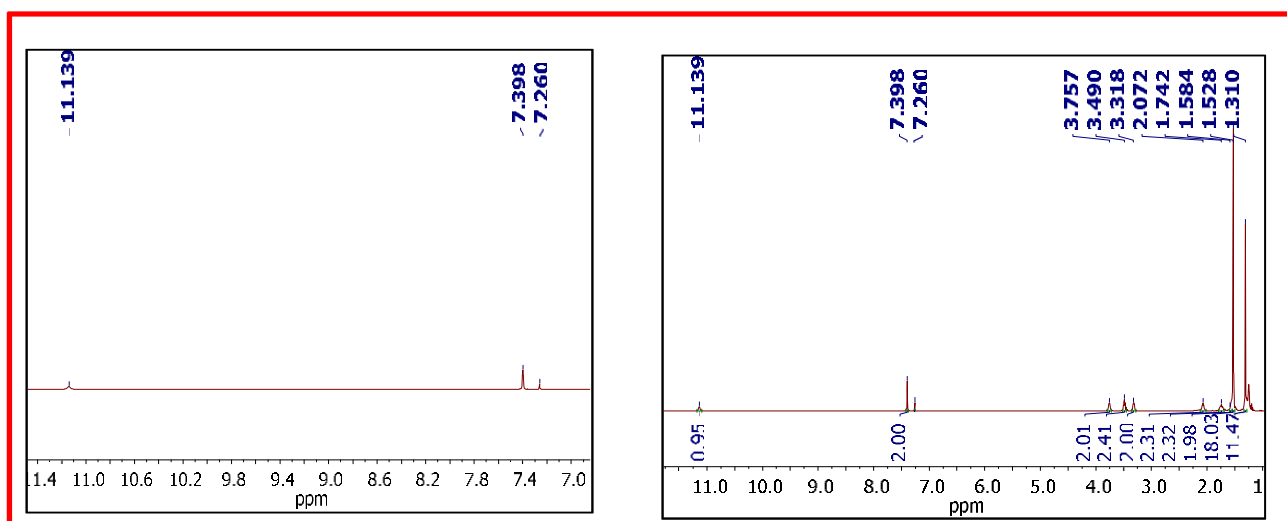
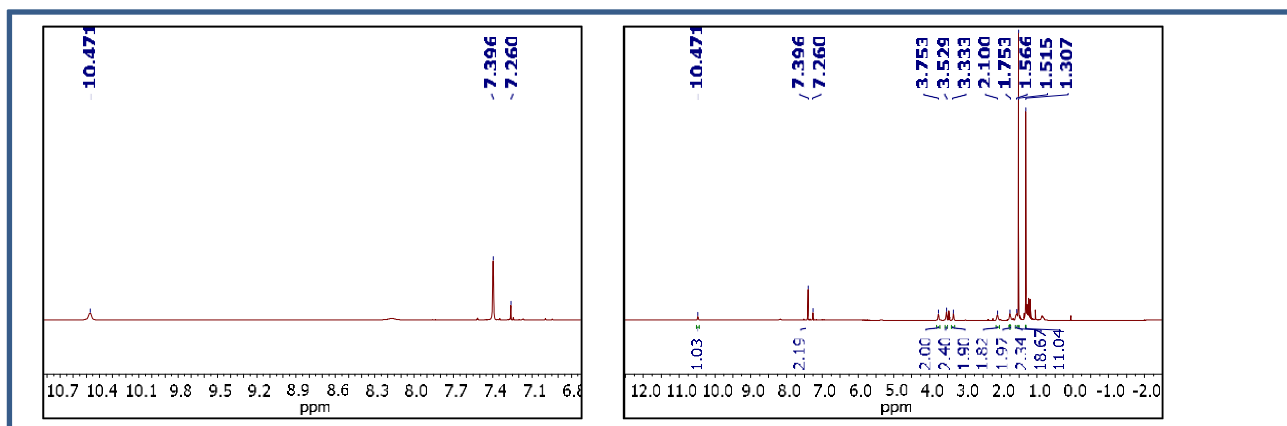
Experiment A. In this case, the spectrum above corresponds to a typical sample of anhydrous **2** in  $\text{CDCl}_3$ . The bottom spectrum corresponds to a sample of **2** carefully titrated with  $\sim 1.1$  equivalents of water using a Hamilton syringe. As can be seen on the top spectrum without water, only a signal at 10.63 ppm corresponding to an N-H interaction is present (blue square), whereas on the bottom spectrum, a signal corresponding to hydrogen-bonded water is downfield shifted to 2.35 ppm (green square) from 1.56 ppm in  $\text{CDCl}_3$  ( $\text{O}6 = 0.79$  ppm); the N-H signal experiences a slight downfield shift to 11.17 ppm ( $\text{O}6 = 0.53$  ppm; red square). The Mes\* aromatic protons show a very light downfield shift from 7.39 to 7.41 ppm in the hydrogen-bonded environment.



Experiment B. Spectra a-c correspond to selected  $^{31}\text{P}$  NMR experiments of  $2\cdot\text{H}_2\text{O}$  after several hours. The experiments were obtained using the same solvent and experimental pulse to improve the comparability of the data. As seen in all three cases, the appearance of low-field (i.e. phosphalkenes; not irreversible impurities as confirmed in other experiments) minor resonances close to region of the main phosphalkene peak suggests a complex dynamic equilibrium typical of HB containing species in solution. Another potential contribution in hand with the observed resonances are phosphonium cations with resonance stabilised hydrogen bonds on the periphery.



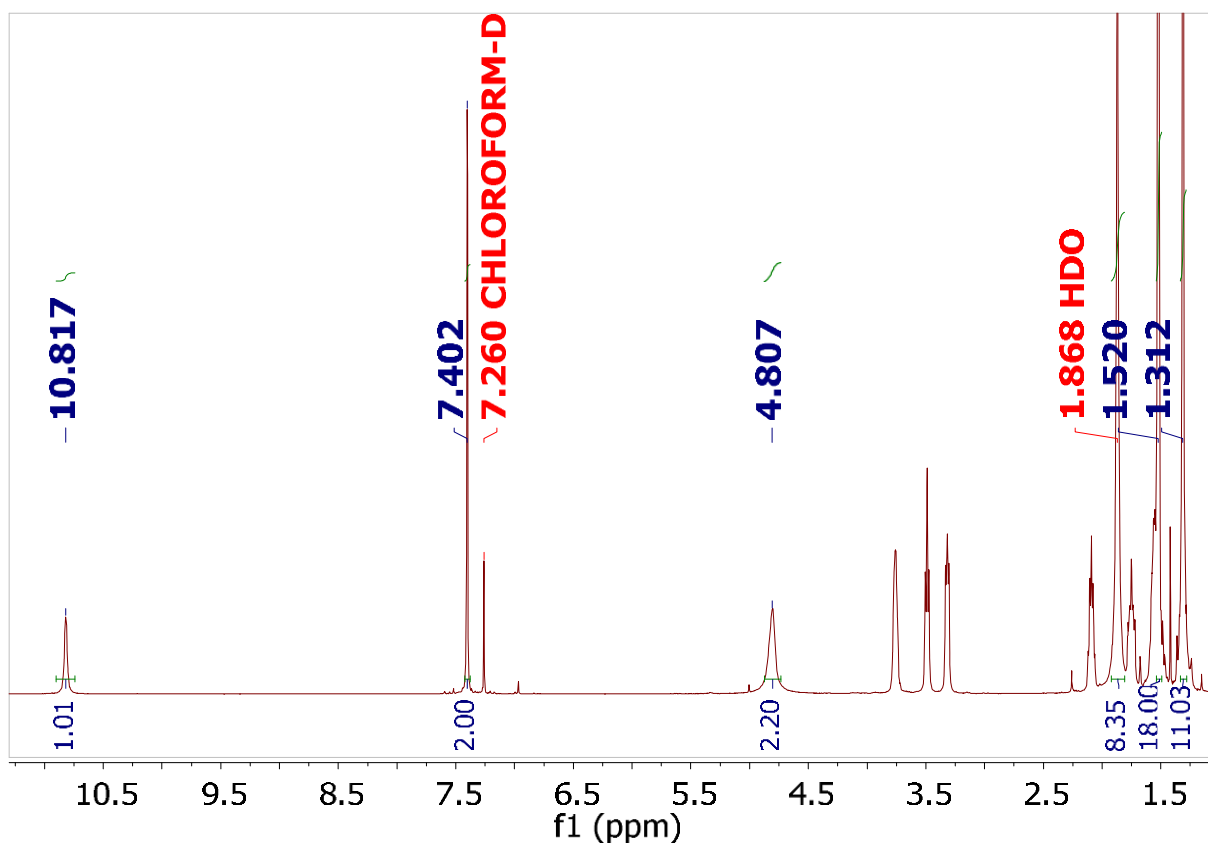
Experiment C.  $^1\text{H}$  NMR spectra of **2** with around one equivalent of  $\text{H}_2\text{O}$ . Spectrum **a**) (expansions are shown in **b**) and **c**). The dynamic character of the signals at 10.435, 6.631, and 4.731 ppm (solvent  $\text{CD}_2\text{Cl}_2$ ), corresponding to  $\text{N}\cdots\text{H}\cdots\text{Cl}$  and the last two to  $\text{Cl}\cdots\text{H}\cdots\text{O}\cdots\text{H}$  and  $\text{H}\cdots\text{O}\cdots\text{H}$  signals, justified by the integrals from **a**) to **c**), and their chemical shifts. The spectrum **d**), expanded in **e**) and **f**), was taken 72 hours later. Based on the NMR tube level markings, less than 5% of the original 0.6 mL of solvent had evaporated, thus the integrations are valid. The downfield shift of the N-H signal to 10.558 ppm and appearance of new signals correspond to increased hydrogen bond character due to a relatively more concentrated solution versus the original experiment and more time in solution to establish a chemical equilibrium, containing more, presumably supramolecular species (see expansion **f**). The upfield shifts of the O-H resonances to 6.433 ppm and almost disappearance of the resulting signal at 4.687 ppm, respectively suggest less hydrogen bonding character of the  $\text{Cl}\cdots\text{H}\cdots\text{O}\cdots\text{H}$  resonances, which could both be related to a simultaneous introduction of  $\text{H}_2\text{O}$  from the atmosphere during the 72 hours, and the inherent increased water exchange, supported by the integrations seen in **f**) as opposed to **c**) initially. In the latter, the OH- resonance at 4.731 ppm, now at 4.687 ppm, has vanished. Spectrum **g**):  $^1\text{H}$ - $^{13}\text{C}$  NMR HSQC showing signals at 10.45, 6.63 ppm do not correspond to carbon bonded impurities.



Experiment D: In experiment D the dynamic N-H signal of **anhydrous 2** is probed in an experiment with ~10 mg of **2** (top spectrum. Top left: expansion. Top right: full spectrum) vs. another one with 12 mg (Bottom spectrum. Bottom left: expansion. Bottom right: full spectrum) in 0.6 mL of  $\text{CDCl}_3$ . Selected spectroscopic features:

Spectrum 1:  $^1\text{H}$  NMR (400 MHz, Chloroform-*d*)  $\delta$  10.471 (N-H, 1H), 7.396 (Mes<sup>\*</sup>-H, 2H), 7.260 ( $\text{CDCl}_3$ ).

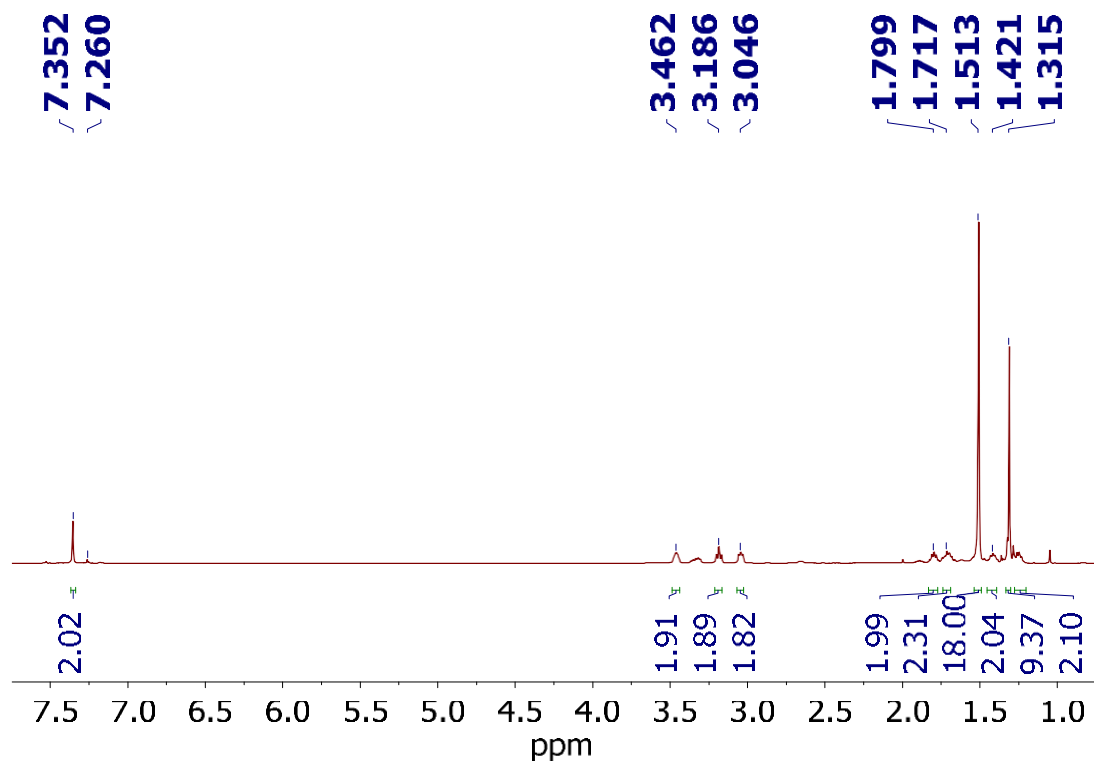
Spectrum 2:  $^1\text{H}$  NMR (400 MHz, Chloroform-*d*)  $\delta$  11.139 (s, 1H), 7.398 (s, 2H), 7.260 ( $\text{CDCl}_3$ ). The mixture of ~20% more **2** experiences a downfield shift of the N-H signal from 10.471 ppm (i.e. Spectrum 1) to 11.139 ppm (i.e. Spectrum 2) typical of increased hydrogen bonding interactions.



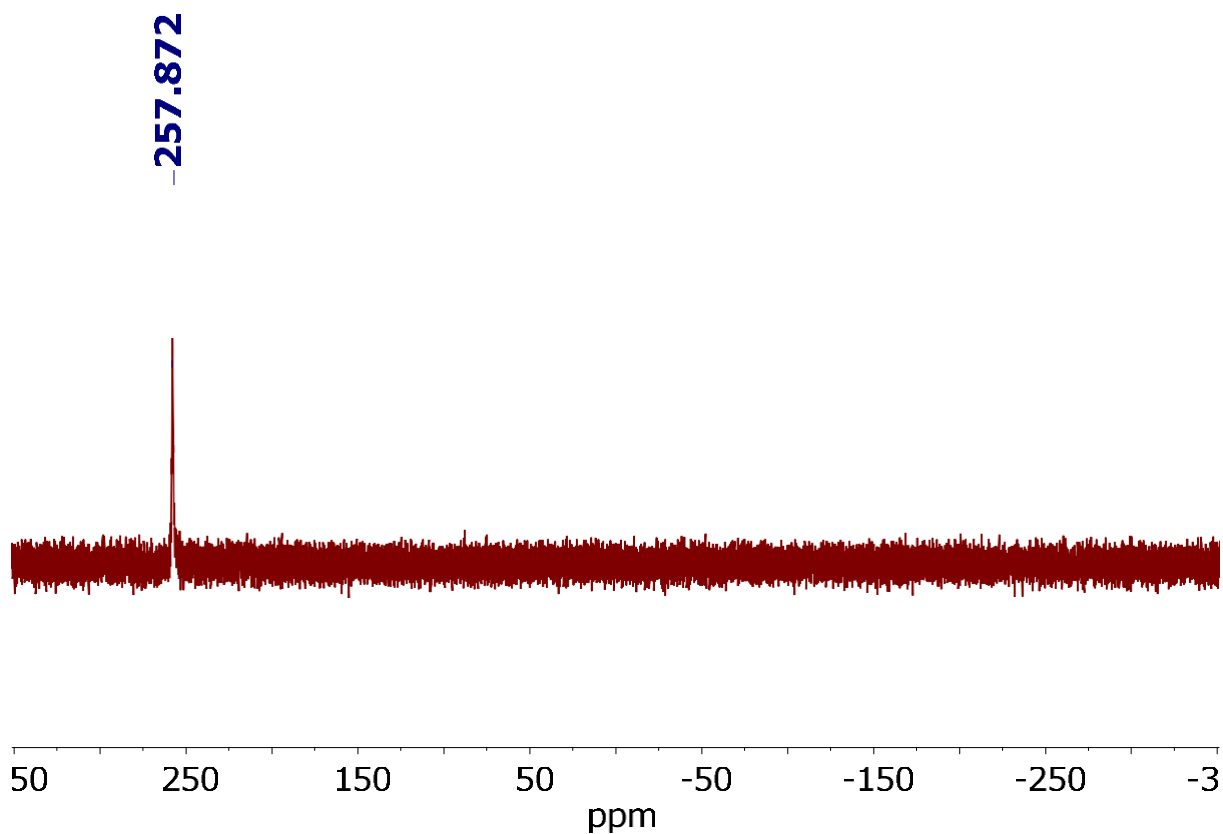
Experiment E: In this experiment, to a solution of **2** (~10 mg) in 0.5 mL of CDCl<sub>3</sub>, around 0.1 ml of a 10 M H<sub>2</sub>O (in THF) mixture (>50 eq. of H<sub>2</sub>O). The excess THF was evaporated. Interestingly, after being under vacuum at  $< 9 \times 10^{-1}$  mbar for 30 minutes with light warming (40 °C), the resulting mixture was a wet paste, suggesting the partial hydrophilicity of this compound. The sample was re-dissolved in CDCl<sub>3</sub>; the “water” signal at 1.87 ppm, which integrate 8 protons in total, i.e. four water molecules per molecule of **2**. Despite the excess water (peak at 4.81 ppm) the relative broad signals in the slow exchange regime NH signal and OH- signals strongly support strongly hydrogen bonded monomeric or dimeric species.

## Selected NMR Spectra

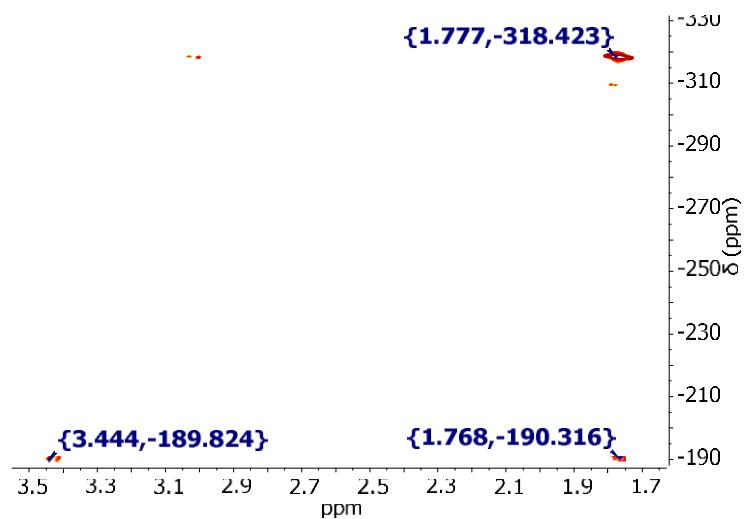
<sup>1</sup>H-NMR Spectrum of 1



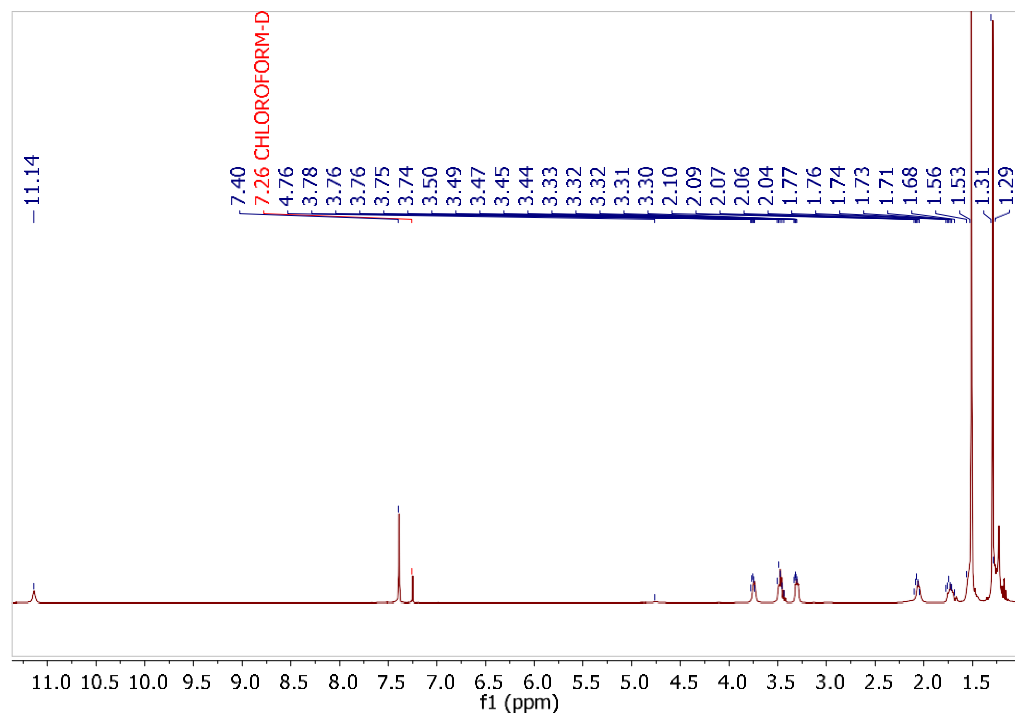
<sup>31</sup>P NMR of 1



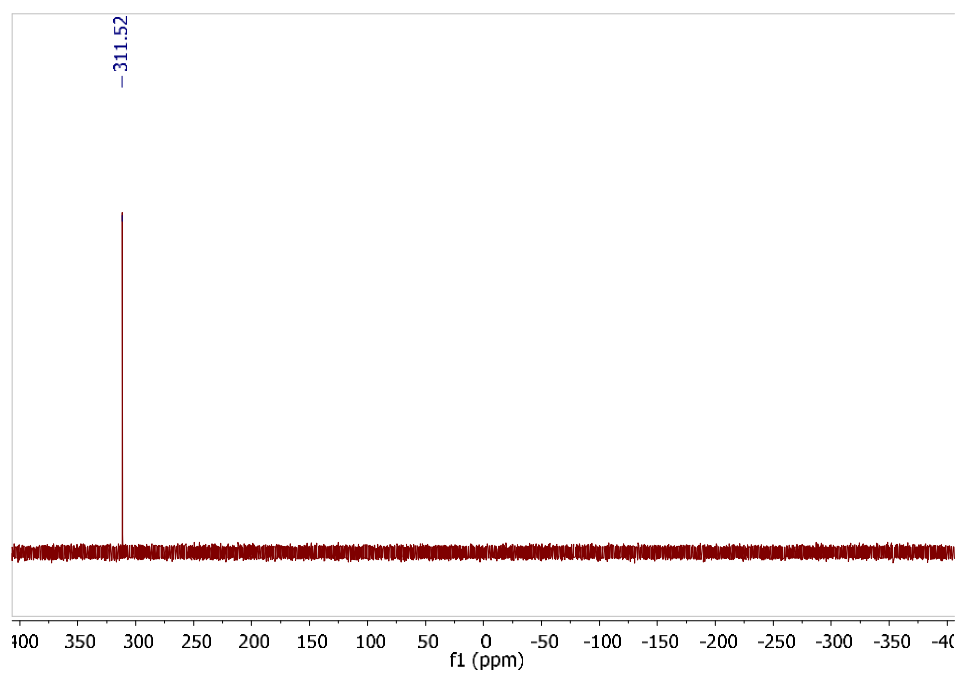
<sup>1</sup>H HMBC- <sup>15</sup>N NMR of 1



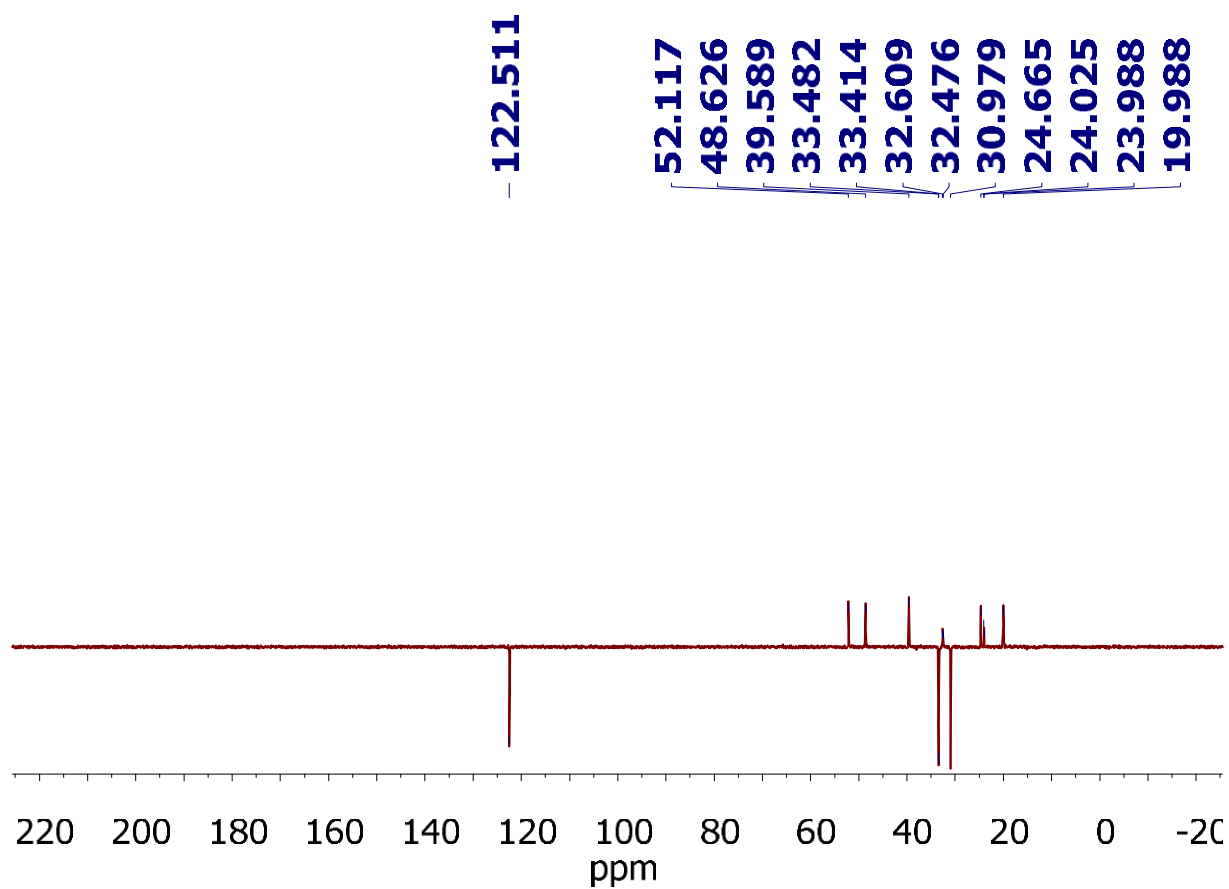
### <sup>1</sup>H-NMR Spectrum of 2



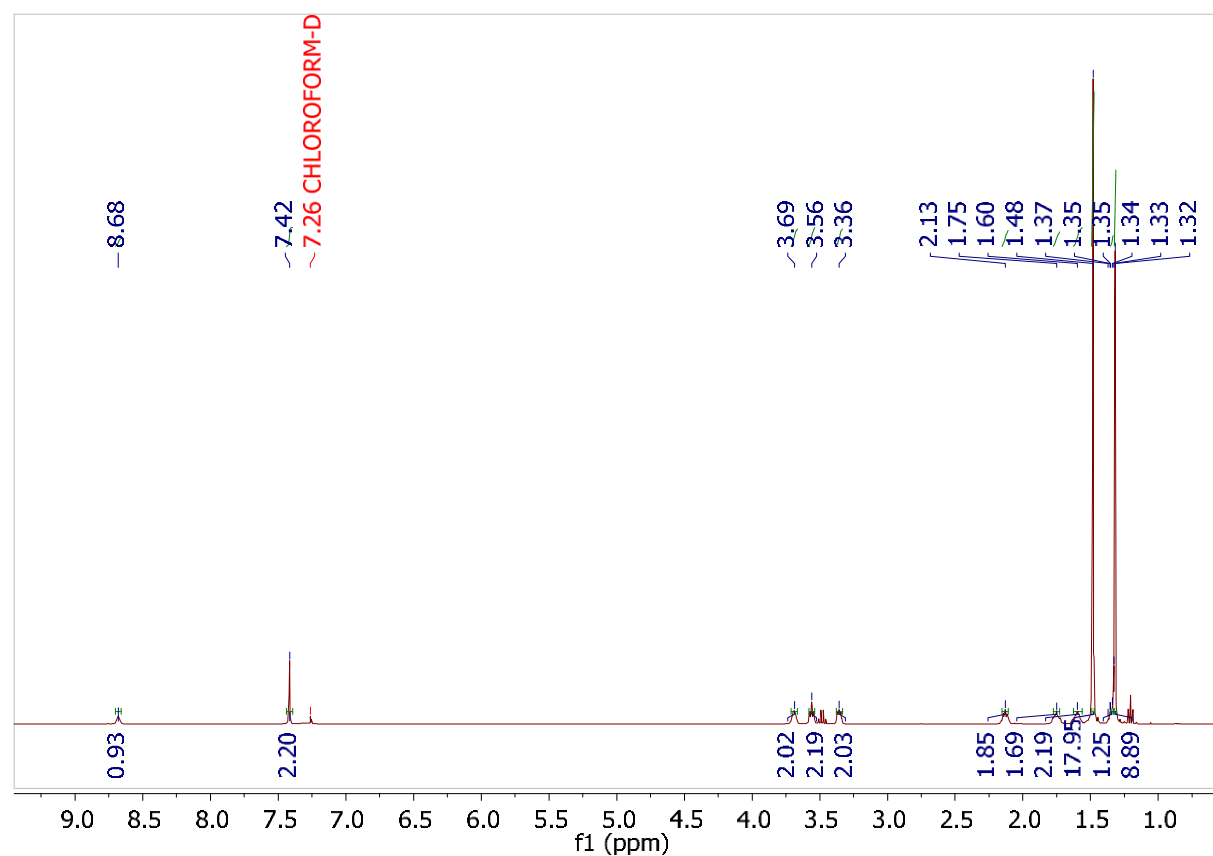
### <sup>31</sup>P-NMR Spectrum of 2



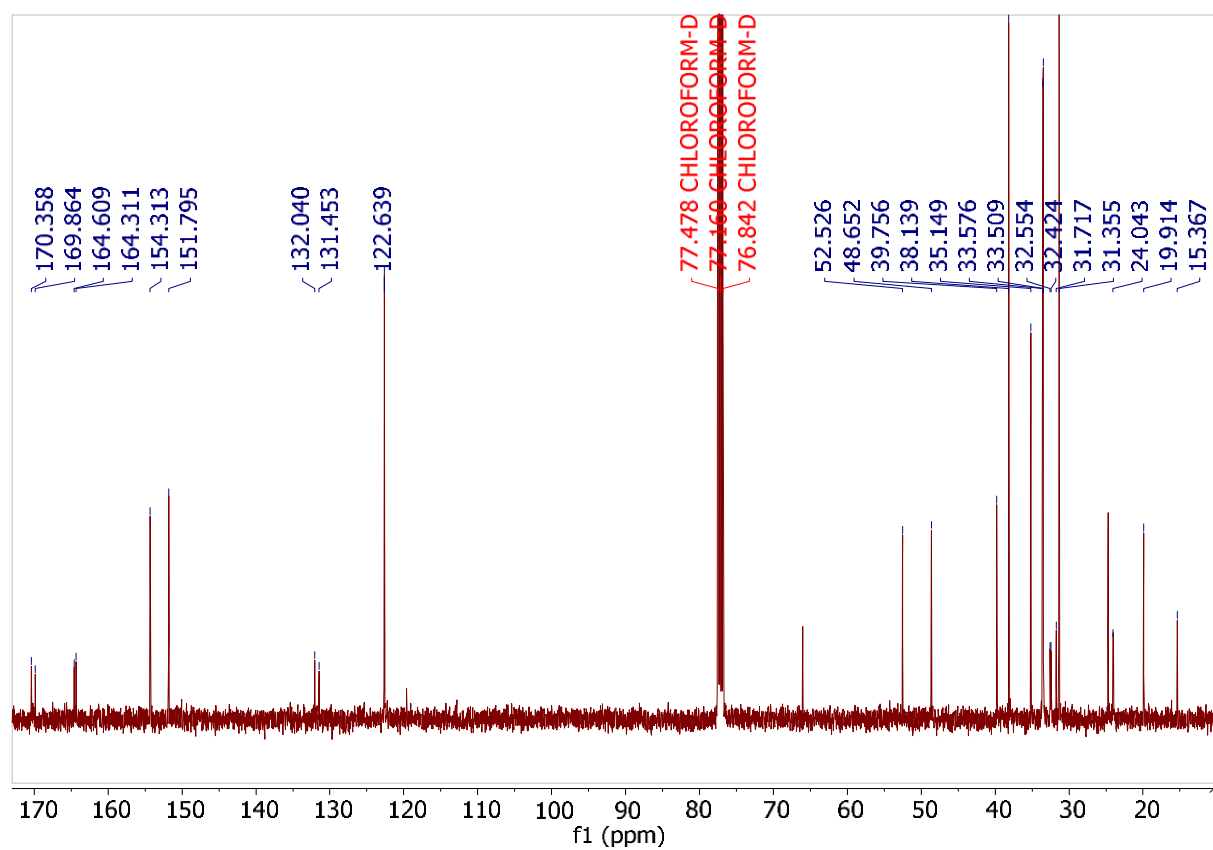
DEPT-135 <sup>13</sup>C-NMR Spectrum of 2



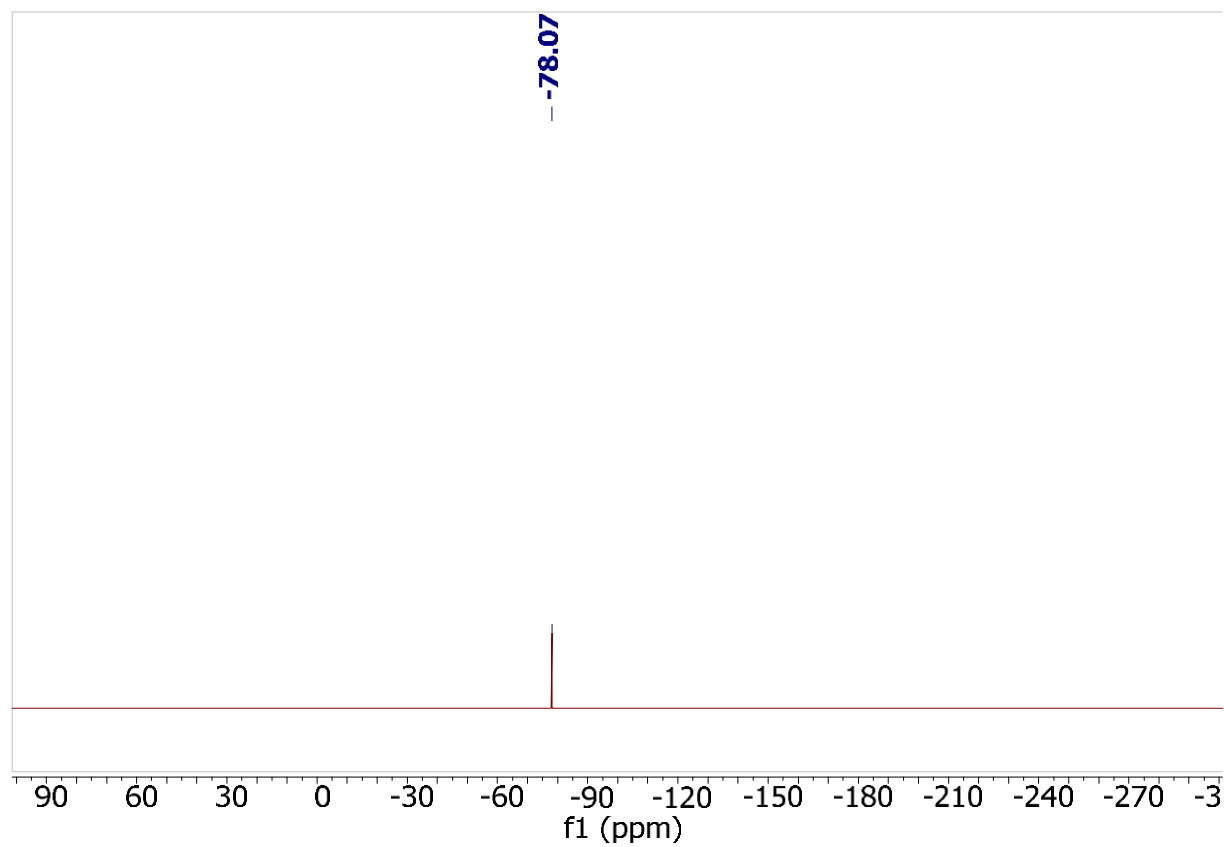
<sup>1</sup>H NMR of 3



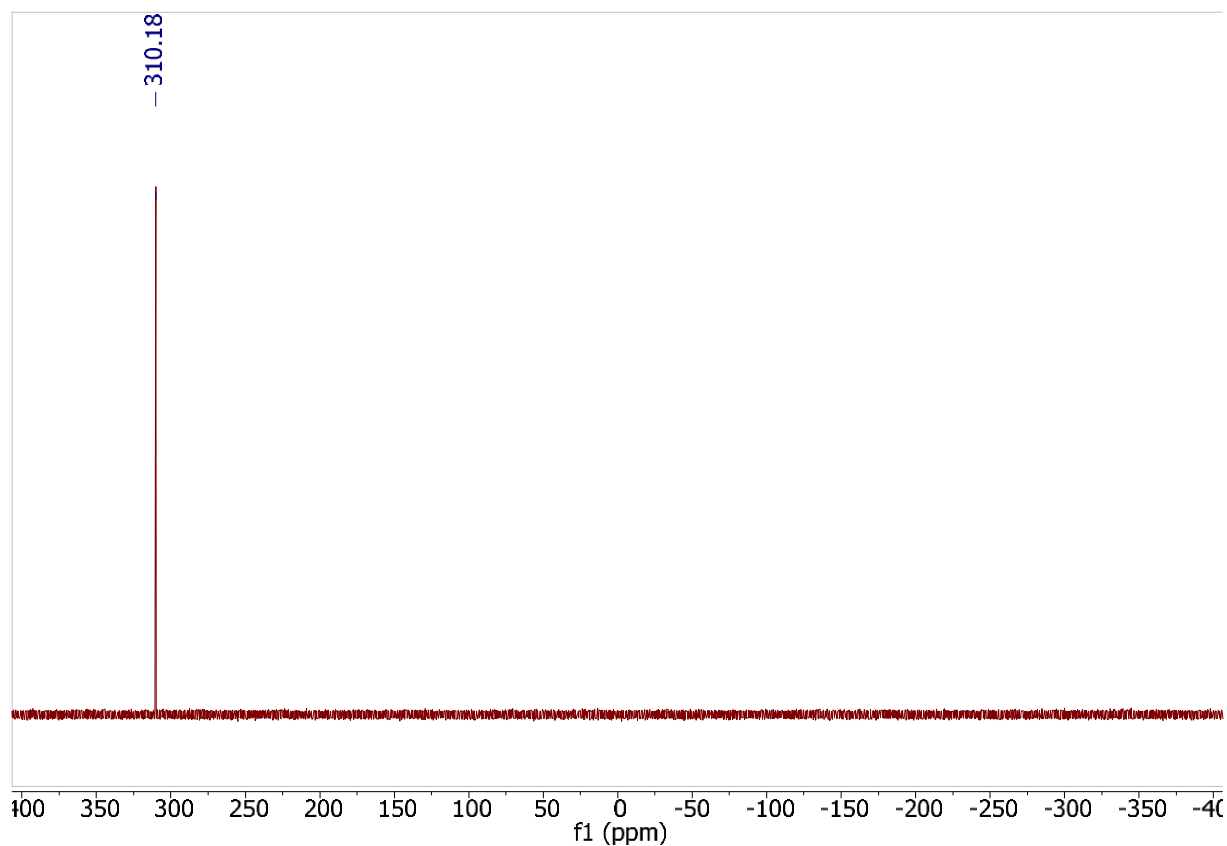
<sup>13</sup>C NMR of 3



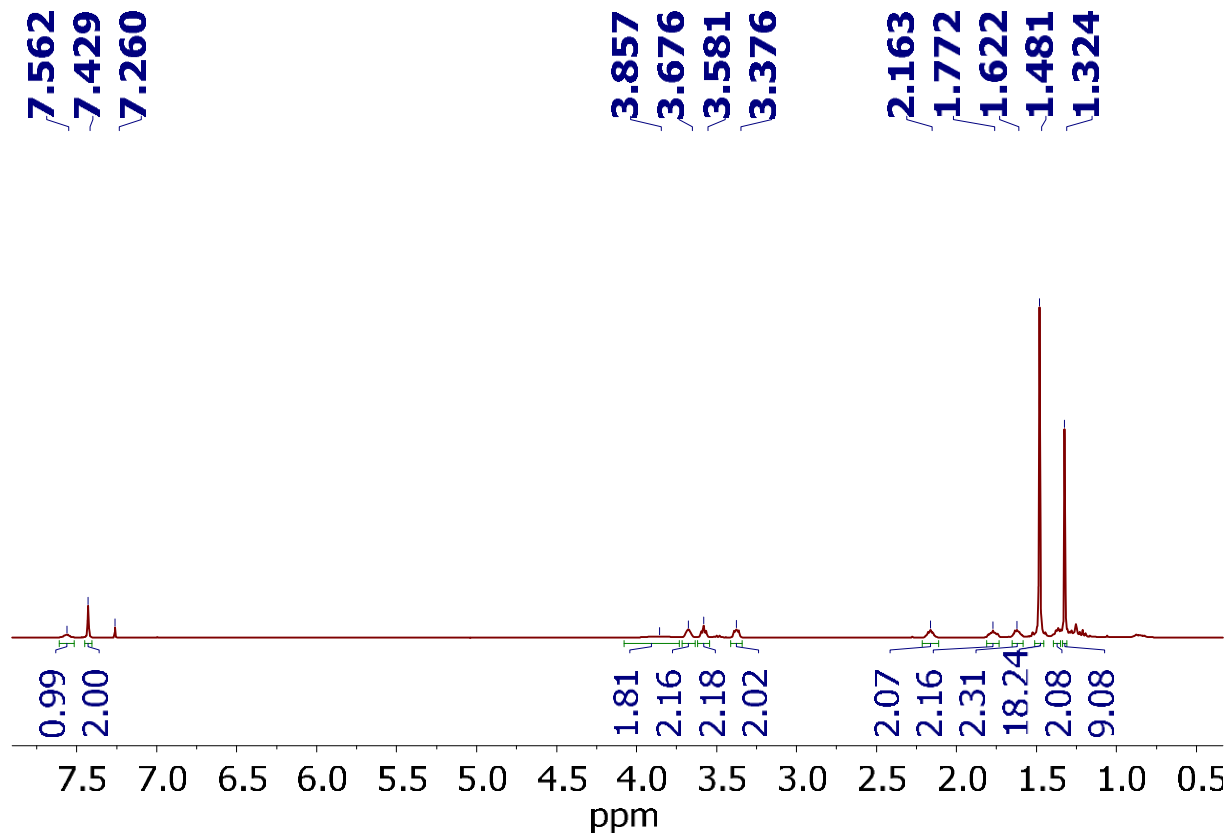
<sup>19</sup>F NMR of 3



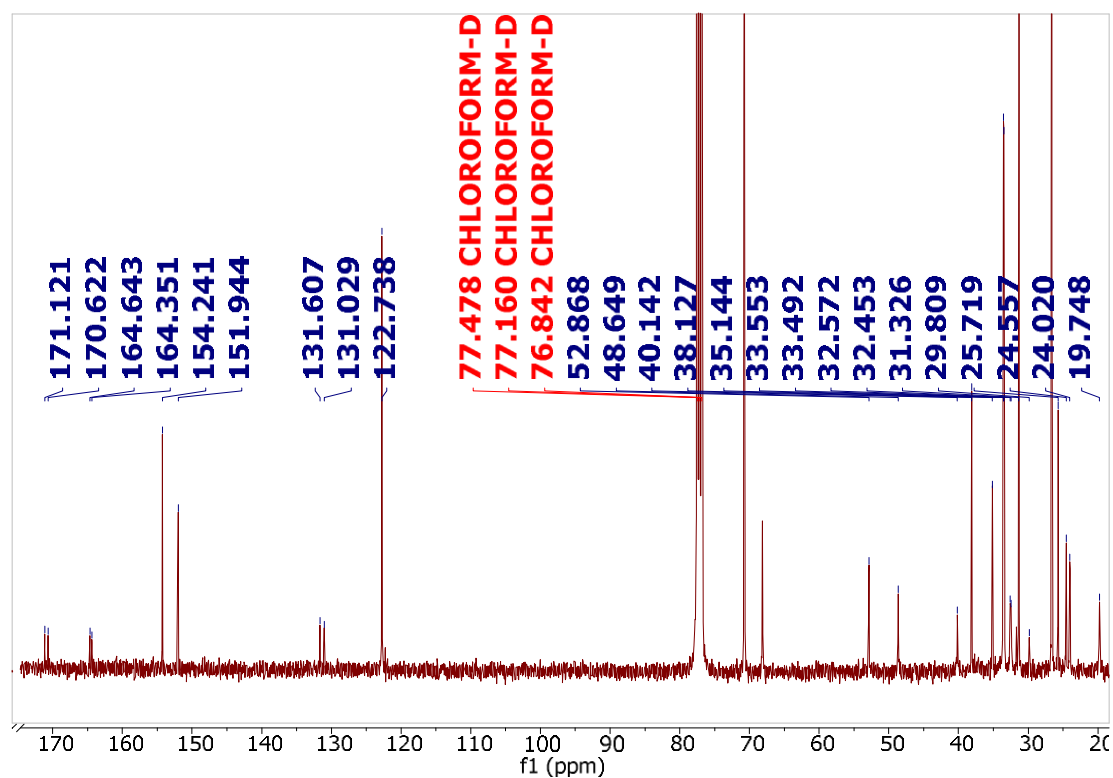
<sup>31</sup>P NMR of 3



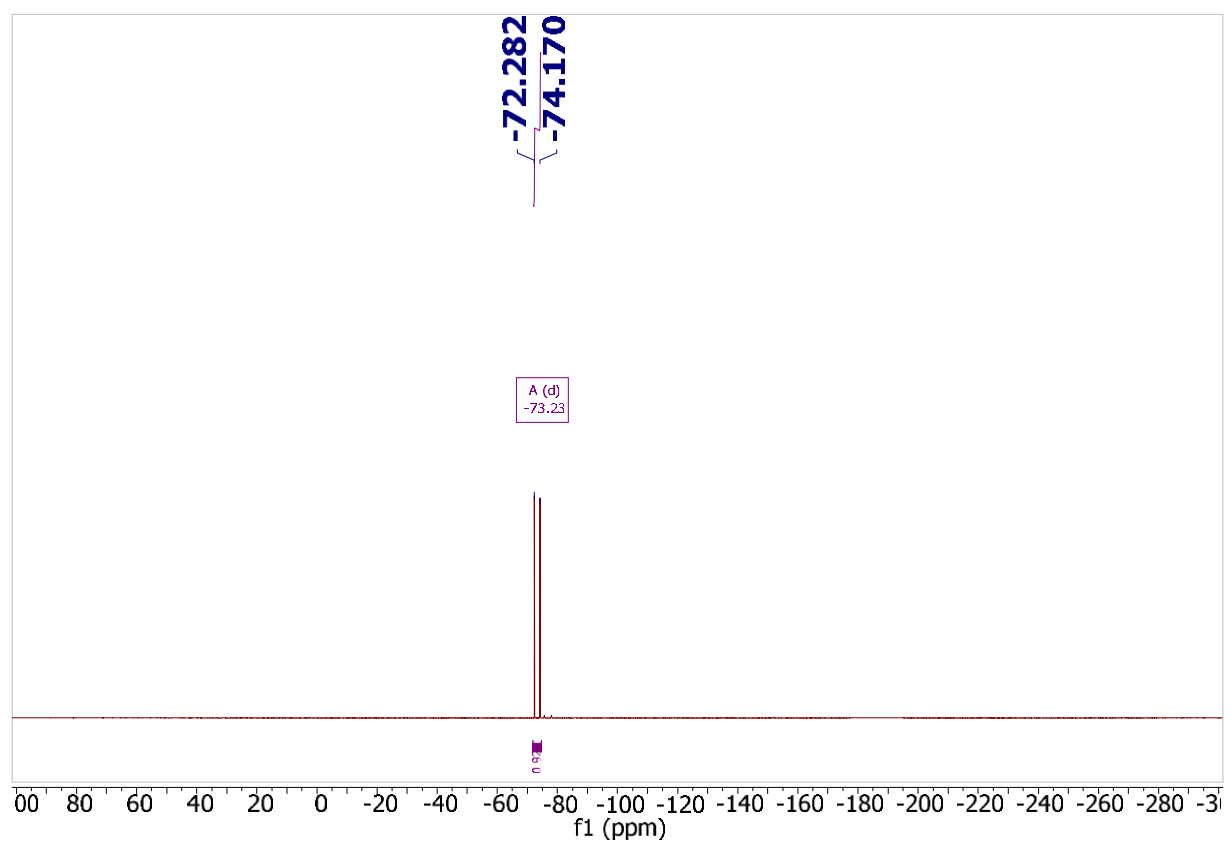
<sup>1</sup>H NMR of 4



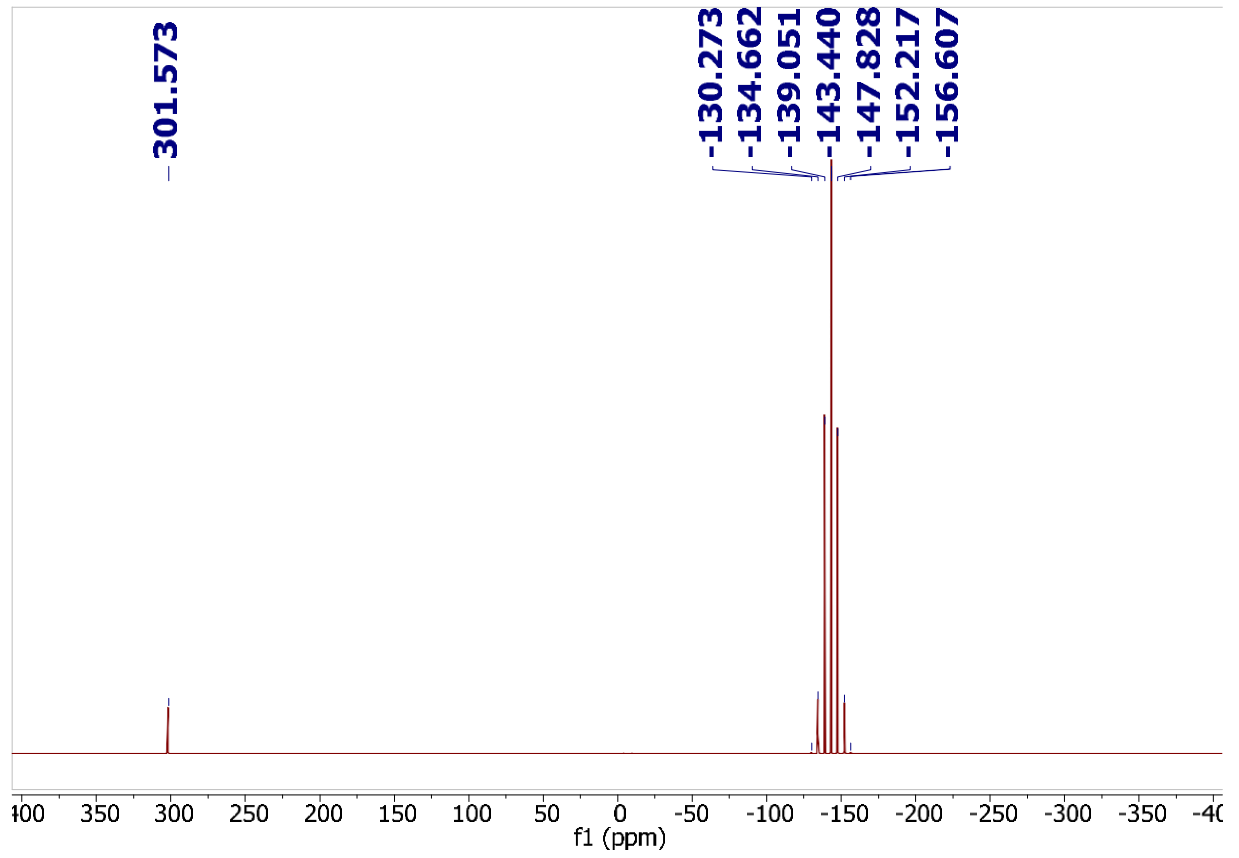
<sup>13</sup>C NMR of 4



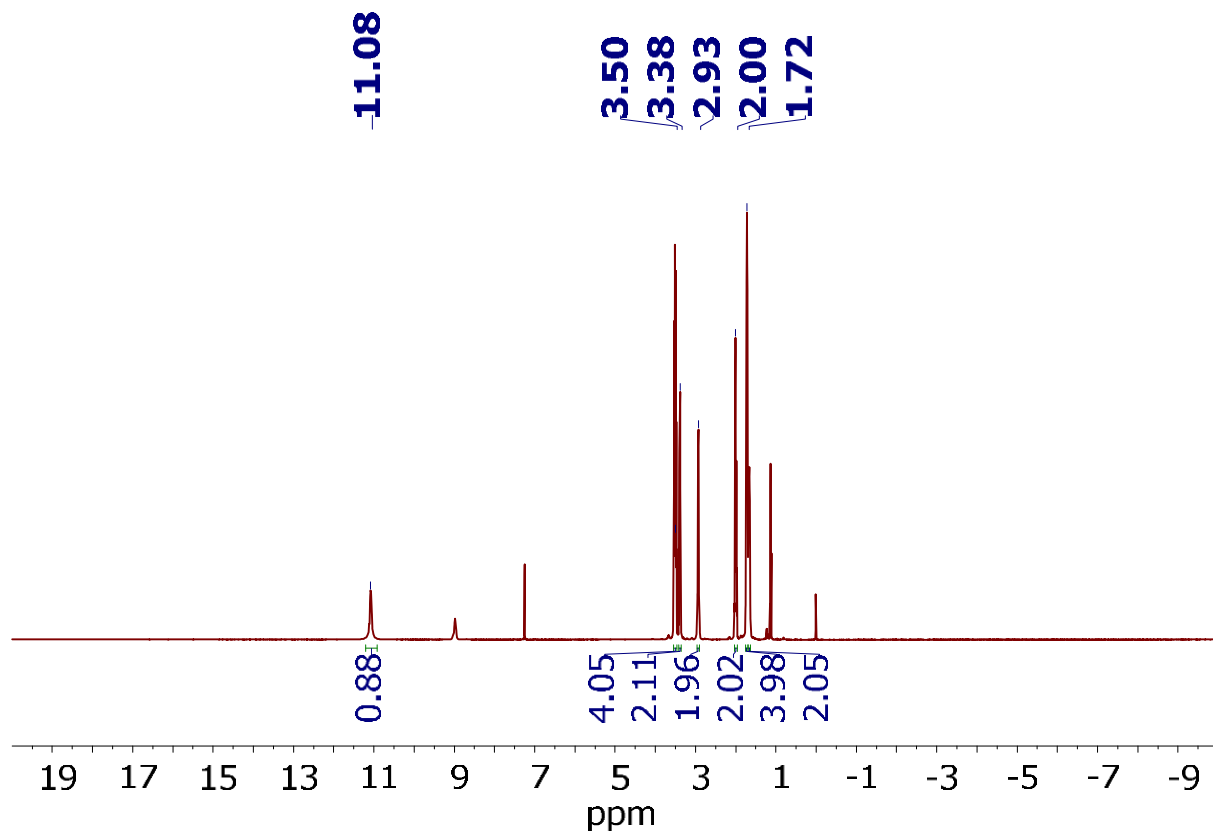
<sup>19</sup>F NMR of 4



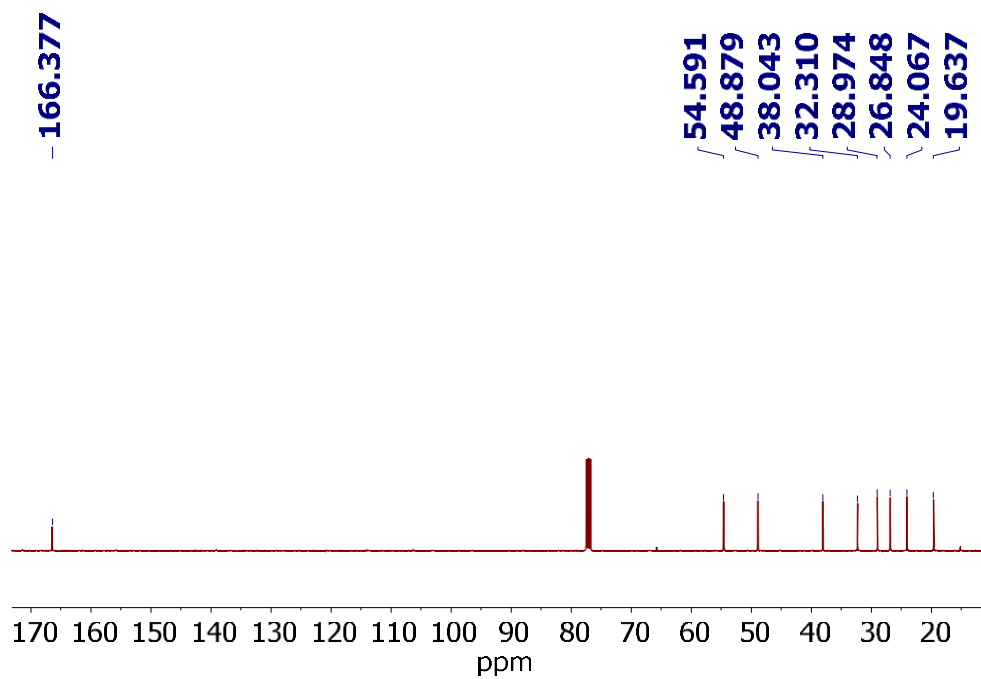
<sup>31</sup>P NMR of 4



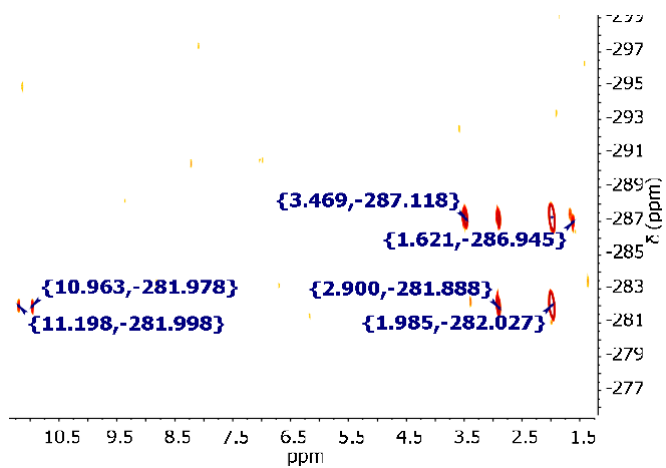
<sup>1</sup>H NMR of 5



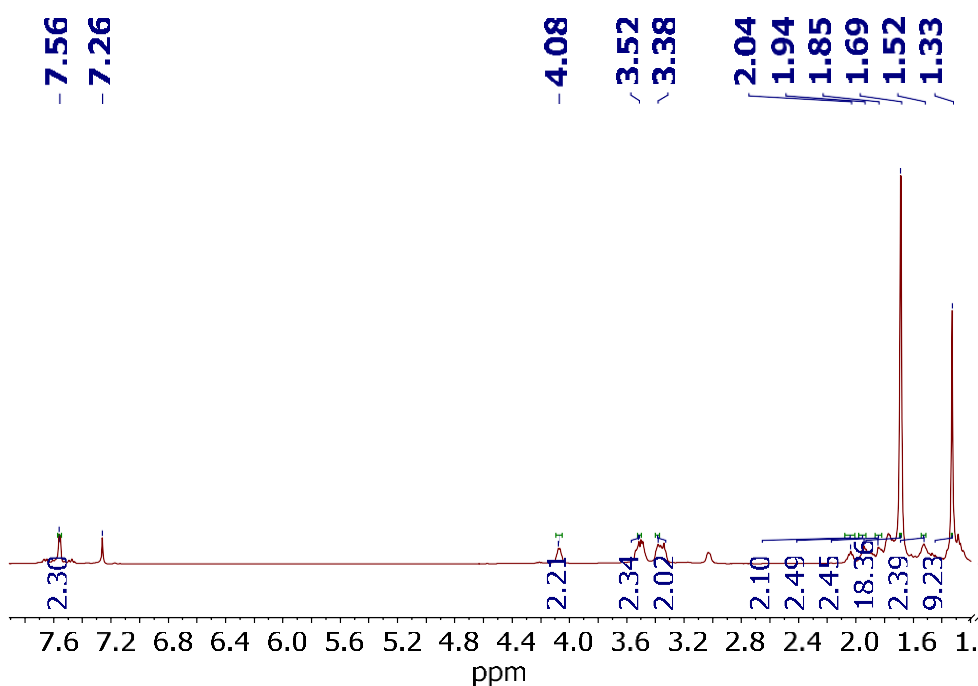
<sup>13</sup>C NMR of 5



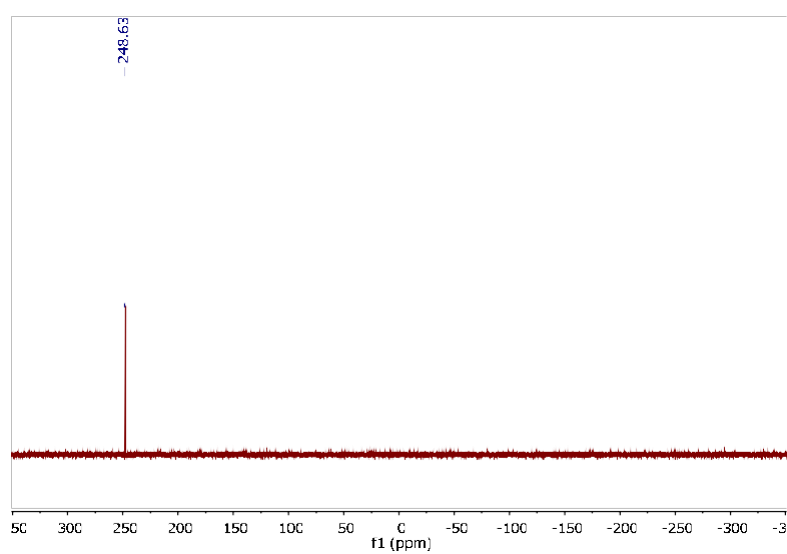
$^1\text{H}$ - $^{15}\text{N}$  NMR HMB(400 MHz) of 5



$^1\text{H}$  NMR of 6



$^{31}\text{P}$  NMR of 6



## SI References

- [1] R. Knorr, C. Pires, C. Behringer, T. Menke, J. Freudenreich, E. C. Rossmann, P. Böhler, *J. Am. Chem. Soc.* **2006**, *128*, 14845-14853.
- [2] Y. Furutani, M. Shibata, H. Kandori, *Photocheml & Photobiol. Sci.* **2005**, *4*, 661-666.
- [3] a) L. D. Quin, E.-Y. Yao, J. Szewczyk, *Tet. Let.* **1987**, *28*, 1077-1080; b) K. Esfandiari, J. Mai, S. Ott, *J. Am. Chem. Soc.* **2017**, *139*, 2940-2943.
- [4] J. M. Chalmers, *Handbook of vibrational spectroscopy* **2006**.
- [5] a) M. Shibata, K. Ihara, H. Kandori, *Biochemistry* **2006**, *45*, 10633-10640; b) L. Delzeit, B. Rowland, J. P. Devlin, *J. Phys. Chem.* **1993**, *97*, 10312-10318; c) L. S. Lussier, C. Sandorfy, H. Le Thanh, D. Vocelle, *J. Phys. Chem.* **1987**, *91*, 2282-2287.

### Single crystal X-ray Crystallography

Reflections were collected on a Bruker APEXII CCD diffractometer using graphite-monochromated MoK $\alpha$  radiation ( $\lambda = 0.71073 \text{ \AA}$ ). Crystals were mounted on the loop. Data reduction was performed with SAINT.<sup>1</sup> Absorption corrections for the area detector were performed using SADABS.<sup>2</sup> Structures were determined by direct methods and refined by least-squares methods on F<sup>2</sup> using the SHELX suit of programs.<sup>3</sup> Non-hydrogen atoms were refined anisotropically. Hydrogen atoms were constrained in geometrical positions to their parent atoms unless otherwise specified.

Compound	1	2·H <sub>2</sub> O	3	4·CHCl <sub>3</sub>
<b>CCDC No.</b>	<b>1828166</b>	<b>1828168</b>	<b>1828165</b>	<b>1828169</b>
Chemical formula	C <sub>27</sub> H <sub>43</sub> N <sub>2</sub> P	C <sub>27</sub> H <sub>46</sub> N <sub>2</sub> OCIP	C <sub>28</sub> H <sub>44</sub> N <sub>2</sub> F <sub>3</sub> O <sub>3</sub> PS	C <sub>55</sub> H <sub>90</sub> F <sub>12</sub> N <sub>4</sub> P <sub>4</sub> Cl <sub>2</sub>
Formula weight	426.60	481.08	576.68	1230.08
Temperature (K)	150(2)	150(2)	150(2)	150(2)
Wavelength (Å)	0.71073 Å	0.71073 Å	0.71073 Å	0.71073 Å
Crystal system	Monoclinic	Monoclinic	Monoclinic	Monoclinic
Space group	P2(1)/c	C2/c	P2(1)/n	P2(1)/c
a (Å); $\alpha$ (°)	14.800(11); 90	37.403(9); 90	17.125(14); 90	28.528(5); 90
b (Å); $\beta$ (°)	10.174(8); 106.39(10)	8.122(2); 107.542(2)	8.582(6); 96.75(5)	8.575(15); 115.543(3)
c (Å); $\gamma$ (°)	17.799(14); 90	19.128(4); 90	20.778(15); 90	27.535(5); 90
V (Å <sup>3</sup> ); Z	2571.1(3); 4	5540.7(2); 8	3032.6(4); 4	6077.4(18); 4
$\rho$ (calc.) g cm <sup>-3</sup>	1.102	1.153	1.263	1.344
$\mu$ (Mo K $\alpha$ ) mm <sup>-1</sup>	0.122	0.216	0.209	0.288
2 $\theta$ <sub>max</sub> (°)	50	50	50	50
R(int)	0.0502	0.0758	0.0695	0.0975
Completeness to $\theta$	99.9 %	100 %	99.1 %	100 %
Data / param.	4656 / 290	5165 / 310	5434 / 412	10694 / 720
GOF	1.028	1.057	1.048	1.045
R1 [F > 4 $\sigma$ (F)]	0.0601	0.0540	0.0705	0.0804
wR2 (all data)	0.1786	0.1681	0.1894	0.2261
max. peak/hole (e.Å <sup>-3</sup> )	0.957 / -0.280	1.139 / -0.410	1.248 / -0.282	0.927 / -0.920
<b>Compound</b>	<b>5</b>	<b>6</b>		
<b>CCDC NO.</b>	<b>1828164</b>	<b>1828167</b>		
Chemical formula	C <sub>9</sub> H <sub>17</sub> N <sub>2</sub> Cl	C <sub>27</sub> H <sub>43</sub> N <sub>2</sub> Cl <sub>2</sub> PPd		
Formula weight	188.69	603.90		
Temperature (K)	150(2)	296(2)		
Wavelength (Å)	0.71073	0.71073 Å		
Crystal system	Orthorhombic	Monoclinic		
Space group	Pna2(1)	P2(1)/c		
a (Å); $\alpha$ (°)	11.598(17); 90	17.607(7); 90		
b (Å); $\beta$ (°)	9.293(14); 90	10.577(4); 96.971(3)		
c (Å); $\gamma$ (°)	9.464(14); 90	15.330(7); 90		
V (Å <sup>3</sup> ); Z	1020.1(3); 4	2833.6(2); 4		
$\rho$ (calc.) g cm <sup>-3</sup>	1.229	1.416		
$\mu$ (Mo K $\alpha$ ) mm <sup>-1</sup>	0.326	0.918		
2 $\theta$ <sub>max</sub> (°)	50	50		
R(int)	0.0480	0.1382		
Completeness to $\theta$	100 %	100 %		
Data / param.	1794 / 109	4988 / 307		
GOF	1.099	1.004		
R1 [F > 4 $\sigma$ (F)]	0.0520	0.0531		
wR2 (all data)	0.1225	0.1353		
max. peak/hole (e.Å <sup>-3</sup> )	0.351 / -0.292	0.749 / -0.441		

(1) SAINT, Bruker AXS Inc. Madison, WI, 2007.

(2) SADABS, Bruker AXS Inc. Madison, WI, 2001.

(3) G. M. Sheldrick, short history of SHELX. Acta Crystallogr., Sect. A: Found. Crystallogr. 2008, 64, 112–122.